

CERN-PH-EP-2012-359

09 December 2012

## Long-range angular correlations on the near and away side in p–Pb collisions at $\sqrt{s_{NN}} = 5.02$ TeV

5

ALICE Collaboration\*

December 1, 2012

DRAFT v0.90 \$Revision: 631 \$

### Abstract

Angular correlations between charged trigger and associated particles are measured by the ALICE detector in p–Pb collisions at a nucleon–nucleon centre-of-mass energy of 5.02 TeV for transverse momentum ranges within  $0.5 < p_{T,assoc} < p_{T,trig} < 4$  GeV/c. The correlations are measured over two units of pseudorapidity and full azimuthal angle in different intervals of event multiplicity, and expressed as associated yield per trigger particle. Two long-range ridge-like structures, one on the near side and one on the away side, are observed when the per-trigger yield obtained in low-multiplicity events is subtracted from the one in high-multiplicity events. The excess on the near-side is qualitatively similar to the one recently reported by the CMS collaboration, while the excess on the away-side is observed for the first time. The two-ridge structure projected onto azimuthal angle is quantified with the second and third Fourier coefficients as well as by near-side and away-side yields and widths. The yields on the near side and on the away side are equal within the uncertainties for all studied event multiplicity and  $p_T$  bins, and the widths show no significant evolution with event multiplicity or  $p_T$ . These findings suggest that the near-side ridge is accompanied by an essentially identical away-side ridge.

---

\*See Appendix A for the list of collaboration members

## 1 Introduction

25 Two-particle correlations are a powerful tool to explore the mechanism of particle production in collisions of hadrons and nuclei at high energy. Such studies involve measuring the distributions of relative angles  $\Delta\phi$  and  $\Delta\eta$  between pairs of particles: a “trigger” particle in a certain transverse momentum  $p_{T,\text{trig}}$  interval and an “associated” particle in a  $p_{T,\text{assoc}}$  interval, where  $\Delta\phi$  and  $\Delta\eta$  are the differences in azimuthal angle  $\phi$  and pseudorapidity  $\eta$  between the two  
30 particles.

In proton–proton (pp) collisions, the correlation at  $(\Delta\phi \approx 0, \Delta\eta \approx 0)$  for  $p_{T,\text{trig}} > 2 \text{ GeV}/c$  is dominated by the “near-side” jet peak, where trigger and associated particles originate from a fragmenting parton, and at  $\Delta\phi \approx \pi$  by the recoil or “away-side” jet [1]. The away-side structure is elongated along  $\Delta\eta$  due to the longitudinal momentum distribution of partons in the colliding  
35 protons. In nucleus–nucleus collisions, the jet-related correlations are modified and additional structures emerge, which persist over a long range in  $\Delta\eta$  on the near side and on the away side [2–14]. The shape of these distributions when decomposed into a Fourier series defined by  $v_n$  coefficients [15] is found to be dominated by contributions from terms with  $n = 2$  and  $n = 3$  [6, 7, 9–14]. The  $v_n$  coefficients are sensitive to the geometry of the initial state of the  
40 colliding nuclei [16, 17] and can be related to the transport properties of the strongly-interacting de-confined matter via hydrodynamic models [18–20].

Recently, measurements in pp collisions at a centre-of-mass energy  $\sqrt{s} = 7 \text{ TeV}$  [21] and in proton–lead (p–Pb) collisions at a nucleon–nucleon centre-of-mass energy  $\sqrt{s_{\text{NN}}} = 5.02 \text{ TeV}$  [22] have revealed long-range ( $2 < |\Delta\eta| < 4$ ) near-side ( $\Delta\phi \approx 0$ ) correlations in events with signifi-  
45 cantly higher-than-average particle multiplicity. Various mechanisms have been proposed to explain the origin of these ridge-like correlations in high-multiplicity pp and p–Pb events. These mechanisms include colour connections forming along the longitudinal direction [23–25], jet-medium induced [26] and multi-parton [27, 28] interactions, and collective effects arising in the high-density system possibly formed in these collisions [29–34].

50 Preliminary results from two-particle correlations in  $\sqrt{s_{\text{NN}}} = 0.2 \text{ GeV}$  d–Au collisions [35] show a strong suppression of the away-side yield at forward rapidity in central collisions. This modification has been interpreted in the framework of “Colour Glass Condensate” models [36] as a saturation effect caused by nonlinear gluon interactions in the high-density regime at small longitudinal parton momentum fraction  $x$ . Similar effects may arise at midrapidity in p–Pb  
55 collisions at  $\sqrt{s_{\text{NN}}} = 5.02 \text{ TeV}$ , where the parton distributions are probed down to  $x < 10^{-3}$ , which is comparable to the relevant range of  $x$  at forward rapidity ( $y \sim 3$ ) at  $\sqrt{s_{\text{NN}}} = 0.2 \text{ TeV}$ .

This letter presents results extracted from two-particle correlation measurements in p–Pb collisions at  $\sqrt{s_{\text{NN}}} = 5.02 \text{ TeV}$ , recorded with the ALICE detector [37] at the Large Hadron Collider (LHC). The correlations are measured over two units of pseudorapidity and full azimuthal  
60 angle as a function of charged-particle multiplicity, and expressed as associated yield per trigger particle. Sections 2 and 3 describe the experimental setup, and the event and track selection, respectively. Details on the definition of the correlation and the per-trigger-particle associated yield are given in Sect. 4. The results of the analysis are discussed in Sect. 5 and a summary is given in Sect. 6.

## 2 Experimental setup

Collisions of proton and lead beams were provided by the LHC during a short pilot run performed in September 2012. The beam energies were 4 TeV for the proton beam and 1.58 TeV per nucleon for the lead beam, resulting in collisions at  $\sqrt{s_{\text{NN}}} = 5.02$  TeV. The nucleon–nucleon centre-of-mass system moved with respect to the ALICE laboratory system with a rapidity of  $-0.465$ , i.e., in the direction of the proton beam. The pseudorapidity in the laboratory system is denoted with  $\eta$  throughout this letter. Results from pp collisions at  $\sqrt{s} = 2.76$  and 7 TeV are shown in comparison to the p–Pb results.

A detailed description of the ALICE detector can be found in Ref. [37]. The main subsystems used in the present analysis are the Inner Tracking System (ITS) and the Time Projection Chamber (TPC), which are operated inside a solenoidal magnetic field of 0.5 T. The ITS consists of six layers of silicon detectors: from the innermost to the outermost, two layers of Silicon Pixel Detector (SPD) with an acceptance of  $|\eta| < 1.4$ , two layers of Silicon Drift Detector (SDD) with  $|\eta| < 0.9$  and two layers of Silicon Strip Detector with  $|\eta| < 0.97$ . The TPC provides an acceptance of  $|\eta| < 0.9$  for tracks which reach the outer radius of the TPC and up to  $|\eta| < 1.5$  for tracks with reduced track length. The VZERO detector, two arrays of 32 scintillator tiles each, covering the full azimuth within  $2.8 < \eta < 5.1$  (VZERO-A) and  $-3.7 < \eta < -1.7$  (VZERO-C), was used for triggering, event selection and event characterization, namely the definition of event classes corresponding to different particle-multiplicity ranges. In p–Pb collisions, the trigger required a signal in either VZERO-A or VZERO-C. In addition, two neutron Zero Degree Calorimeters (ZDCs) located at +112.5 m (ZNA) and –112.5 m (ZNC) from the interaction point are used in the event selection. The energy deposited in the ZNA, which for the beam setup of the pilot run originates from neutrons of the Pb nucleus, served as an alternative approach in defining the event-multiplicity classes. In pp collisions, the trigger required a signal in either SPD, VZERO-A or VZERO-C [38].

## 3 Event and track selection

The present analysis of the p–Pb data is based on the event selection described in Ref. [39]. The events are selected by requiring a signal in both VZERO-A and VZERO-C. From the data collected,  $1.7 \times 10^6$  events pass the event selection criteria and are used for this analysis. For the analysis of the pp collisions, the event selection described in Ref. [38] has been used, yielding  $31 \times 10^6$  and  $85 \times 10^6$  events at  $\sqrt{s} = 2.76$  and 7 TeV, respectively.

The primary-vertex position is determined with tracks reconstructed in the ITS and TPC as described in Ref. [40]. The vertex reconstruction algorithm is fully efficient for events with at least one reconstructed track within  $|\eta| < 1.4$ . An event is accepted if the coordinate of the reconstructed vertex along the beam direction ( $z_{\text{vtx}}$ ) is within  $\pm 10$  cm from the detector centre.

The analysis uses tracks reconstructed in the ITS and TPC with  $0.5 < p_{\text{T}} < 4$  GeV/ $c$  and in a fiducial region  $|\eta| < 1.2$ . As a first step in the track selection, cuts on the number of space points and the quality of the track fit in the TPC are applied. Tracks are further required to have a distance of closest approach to the reconstructed vertex smaller than 2.4 cm and 3.2 cm in the transverse and the longitudinal direction, respectively. In order to avoid an azimuthally-dependent tracking efficiency due to inactive SPD modules, two classes of tracks are combined [41]. The first class consists of tracks, which have at least one hit in the SPD. The tracks from the second

class do not have any SPD hit associated, but the position of the reconstructed primary vertex is used in the fit of the tracks. In the study of systematic uncertainties an alternative track selection [42] is used, where a tighter  $p_T$ -dependent cut on the distance of closest approach to the reconstructed vertex is applied. Further, the selection for the tracks in the second class is changed to tracks, which have a hit in the first layer of the SDD. This modified selection has a less uniform azimuthal acceptance, but includes a smaller number of secondary particles from interactions in the detector material or weak decays.

The efficiency and purity of the primary charged-particle selection are estimated from a Monte Carlo (MC) simulation using the DPMJET event generator [43] (for p–Pb) and the PYTHIA 6.4 event generator [44] with the tune Perugia-0 [45] (for pp) with particle transport through the detector using GEANT3 [46]. In p–Pb collisions, the combined efficiency and acceptance for the track reconstruction in  $|\eta| < 0.9$  is about 82% at  $p_T = 0.5\text{--}1$  GeV/ $c$ , and decreases to about 79% at  $p_T = 4$  GeV/ $c$ . It reduces to about 50% at  $|\eta| \approx 1.2$  and is independent of the event multiplicity. The remaining contamination from secondary particles due to interactions in the detector material or weak decays decreases from about 2% to 1% in the  $p_T$  range from 0.5 to 4 GeV/ $c$ . The contribution from fake tracks is negligible. These fractions are similar in the analysis of pp collisions.

In order to study the multiplicity dependence of the two-particle correlations the selected event sample is divided into four event classes. These classes are defined fractions of the analyzed event sample, based on cuts on the total charge deposited in the VZERO detector (V0M), and denoted “60–100%”, “40–60%”, “20–40%”, “0–20%” from the lowest to the highest multiplicity in the following. Table 1 shows the event-classes definitions and the corresponding mean charged-particle multiplicity densities ( $\langle dN_{\text{ch}}/d\eta \rangle$ ) within  $|\eta| < 0.5$ . These are obtained using the method presented in Ref. [39], and are corrected for vertex reconstruction efficiency, acceptance and tracking efficiency as well as contamination by secondary particles. Also shown are the mean numbers of primary charged particles with  $p_T > 0.5$  GeV/ $c$  within the pseudorapidity range  $|\eta| < 1.2$ . These are measured by applying the track selection described above and are corrected for the detector acceptance, track-reconstruction efficiency and contamination.

Event class	V0M range (a.u.)	$\langle dN_{\text{ch}}/d\eta \rangle_{ \eta  < 0.5}$ $p_T > 0$ GeV/ $c$	$\langle N_{\text{trk}} \rangle_{ \eta  < 1.2}$ $p_T > 0.5$ GeV/ $c$
60–100%	< 138	$6.7 \pm 0.2$	$6.4 \pm 0.2$
40–60%	138–216	$16.2 \pm 0.4$	$16.9 \pm 0.6$
20–40%	216–318	$23.7 \pm 0.5$	$26.1 \pm 0.9$
0–20%	> 318	$34.9 \pm 0.5$	$42.5 \pm 1.5$

**Table 1:** Definition of the event classes as fractions of the analyzed event sample and their corresponding  $\langle dN_{\text{ch}}/d\eta \rangle$  within  $|\eta| < 0.5$  and the mean numbers of charged particles within  $|\eta| < 1.2$  and  $p_T > 0.5$  GeV/ $c$ . The given uncertainties are systematic while the statistical uncertainties are negligible.

## 4 Analysis

For a given event class, the two-particle correlation between pairs of trigger and associated charged particles is measured as a function of the azimuthal difference  $\Delta\phi$  (defined within  $-\pi/2$  and  $3\pi/2$ ) and pseudorapidity difference  $\Delta\eta$ . The correlation is expressed in terms of the associated yield per trigger particle for different intervals of trigger and associated transverse momentum,  $p_{T,\text{trig}}$  and  $p_{T,\text{assoc}}$ , respectively, and  $p_{T,\text{assoc}} < p_{T,\text{trig}}$ . The associated yield per

trigger particle is defined as

$$\frac{1}{N_{\text{trig}}} \frac{d^2 N_{\text{assoc}}}{d\Delta\eta d\Delta\phi} = \frac{S(\Delta\eta, \Delta\phi)}{B(\Delta\eta, \Delta\phi)} \quad (1)$$

where  $N_{\text{trig}}$  is the total number of trigger particles in the event class and  $p_{T,\text{trig}}$  interval. The signal distribution  $S(\Delta\eta, \Delta\phi) = 1/N_{\text{trig}} d^2 N_{\text{same}}/d\Delta\eta d\Delta\phi$  is the associated yield per trigger particle for particle pairs from the same event. In a given event class and  $p_T$  interval, the sum over  
 145 the events is performed separately for  $N_{\text{trig}}$  and  $d^2 N_{\text{same}}/d\Delta\eta d\Delta\phi$  before their ratio is computed. Note, that this definition is different from the one used in Ref. [22], where  $S(\Delta\eta, \Delta\phi)$  is calculated per event and then averaged. The method used in this letter does not induce an inherent multiplicity dependence in the pair yields, which is important for the subtraction method discussed in the next Section. The background distribution  $B(\Delta\eta, \Delta\phi) = \alpha d^2 N_{\text{mixed}}/d\Delta\eta d\Delta\phi$   
 150 corrects for pair acceptance and pair efficiency. It is constructed by correlating the trigger particles in one event with the associated particles from other events in the same event class and within the same 2 cm wide  $z_{\text{vtx}}$  interval (each event is mixed with 5–20 events). The factor  $\alpha$  is chosen to normalize the background distribution such that it is unity for pairs where both particles are going into approximately the same direction (i.e.  $\Delta\phi \approx 0, \Delta\eta \approx 0$ ). To account  
 155 for different pair acceptance and pair efficiency as a function of  $z_{\text{vtx}}$ , the yield defined by Eq. 1 is constructed for each  $z_{\text{vtx}}$  interval. The final per-trigger yield is obtained by calculating the weighted average of the  $z_{\text{vtx}}$  intervals.

When constructing the signal and background distributions, the trigger and associated particles are required to be separated by  $|\Delta\phi_{\text{min}}^*| > 0.02$  and  $|\Delta\eta| > 0.02$ , where  $\Delta\phi_{\text{min}}^*$  is the minimal  
 160 azimuthal distance at the same radius between the two tracks within the active detector volume after accounting for the bending due to the magnetic field. This procedure is applied to avoid a bias due to the reduced efficiency for pairs with small opening angles and leads to an increase in the associated near-side peak yield of 0.4–0.8% depending on  $p_T$ . Further, particle pairs are removed which are likely to stem from a  $\gamma$ -conversion, or a  $K_s^0$  or  $\Lambda$  decay, by a cut on the  
 165 invariant mass of the pair (the electron, pion, or pion/proton mass is assumed, respectively). The effect on the peak yields is less than 2%.

In the signal as well as in the background distribution, each trigger and each associated particle is weighted with a correction factor accounting for detector acceptance, reconstruction efficiency and contamination by secondary particles. These corrections are applied as a func-  
 170 tion of  $\eta$ ,  $p_T$  and  $z_{\text{vtx}}$ . Applying the correction factors extracted from DPMJET simulations to events simulated with HIJING [47] leads to associated peak yields that agree within 4% with the MC truth. This difference between the two-dimensional corrected per-trigger yield and input per-trigger yield is used in the estimate of the systematic uncertainties. Uncertainties due to track-quality cuts are evaluated by comparing the results of two different track selections, see  
 175 Sect. 3. The associated yields are found to be insensitive to these track selections within 5%. Further systematic uncertainties related to specific observables are mentioned below.

## 5 Results

The associated yield per trigger particle in  $\Delta\phi$  and  $\Delta\eta$  is shown in Fig. 1 for pairs of charged particles with  $2 < p_{T,\text{trig}} < 4 \text{ GeV}/c$  and  $1 < p_{T,\text{assoc}} < 2 \text{ GeV}/c$  in p–Pb collisions at  $\sqrt{s_{\text{NN}}} = 5.02 \text{ TeV}$   
 180 in the 60–100% (left) and 0–20% (right) event classes. In the 60–100% class, the visible features are the correlation peak near  $(\Delta\phi \approx 0, \Delta\eta \approx 0)$  for pairs of particles originating from the

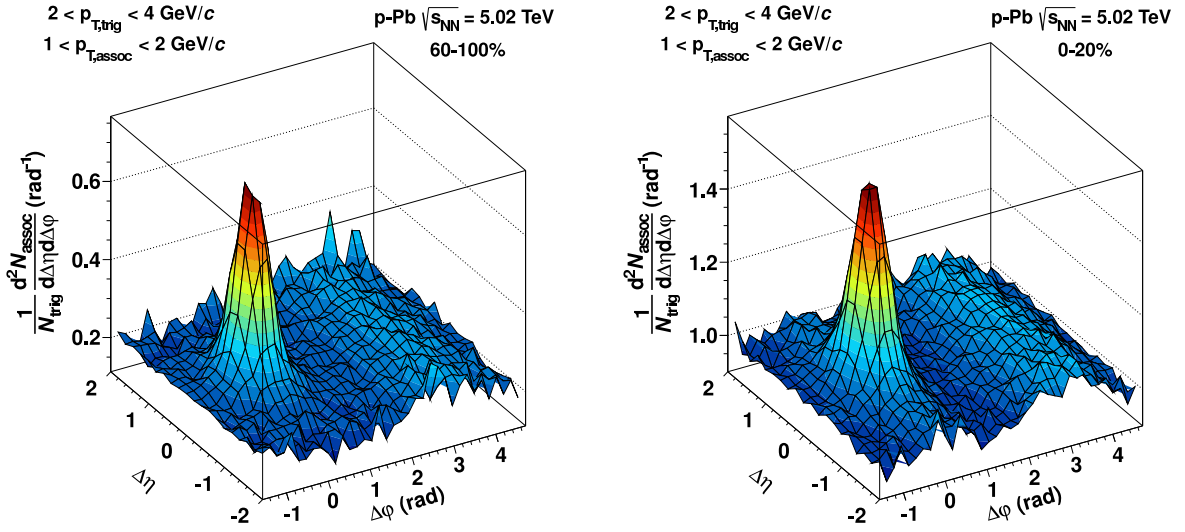


**Fig. 1:** The associated yield per trigger particle in  $\Delta\phi$  and  $\Delta\eta$  for pairs of charged particles with  $2 < p_{T,\text{trig}} < 4$  GeV/c and  $1 < p_{T,\text{assoc}} < 2$  GeV/c in p–Pb collisions at  $\sqrt{s_{NN}} = 5.02$  TeV for the 60–100% (left) and 0–20% (right) event classes.

same jet, and the elongated structure at  $\Delta\phi \approx \pi$  for pairs of particles from jets back-to-back in azimuth. These are very similar to those observed in pp collisions at  $\sqrt{s} = 2.76$  and 7 TeV. The same features are visible in the 0–20% class. However, both the yields on the near side ( $|\Delta\phi| < \pi/2$ ) and the away side ( $\pi/2 < \Delta\phi < 3\pi/2$ ) are higher.<sup>1</sup> This is illustrated in Fig. 2, where the projections on  $\Delta\phi$  averaged over  $|\Delta\eta| < 1.8$  are compared for different event classes and to pp collisions at 2.76 and 7 TeV. In order to facilitate the comparison, the yield at  $\Delta\phi = 1.3$  has been simply subtracted for each distribution. It is seen that the per-trigger yields in  $\Delta\phi$  on the near side and on the away side are similar for low-multiplicity p–Pb collisions and for pp collisions at  $\sqrt{s} = 7$  TeV, and increases with increasing multiplicity in p–Pb collisions.

To quantify the change from low to high multiplicity event classes, we subtract the per-trigger yield of the lowest (60–100%) from that of the higher multiplicity classes. The resulting distribution in  $\Delta\phi$  and  $\Delta\eta$  for the 0–20% event class is shown in Fig. 3 left. A distinct excess structure in the correlation is observed, which forms two ridges, one on the near side and one on the away side. The ridge on the near-side is qualitatively similar to the one recently reported by the CMS collaboration [22]. Note, however that a quantitative comparison would not be meaningful due to the different definition of the per-trigger yield and the different detector acceptance and event-class definition.

On the near side, there is a peak around ( $\Delta\phi \approx 0$ ,  $\Delta\eta \approx 0$ ) indicating a small change of the near-side jet yield as a function of multiplicity. The integral of this peak above the ridge within  $|\Delta\eta| < 0.5$  corresponds to about 5–25% of the unsubtracted near-side peak yield, depending on  $p_T$ . In order to avoid a bias on the associated yields due to the multiplicity selection and to prevent that this remaining peak contributes to the ridge yields calculated below, the region  $|\Delta\eta| < 0.8$  on the near side is excluded when performing projections onto  $\Delta\phi$ . The effect of this incomplete subtraction, which if jet-related might also be present on the away side, on the extracted observables is discussed further below.

<sup>1</sup>These definitions of near-side ( $|\Delta\phi| < \pi/2$ ) and away-side ( $\pi/2 < \Delta\phi < 3\pi/2$ ) are used throughout the letter.

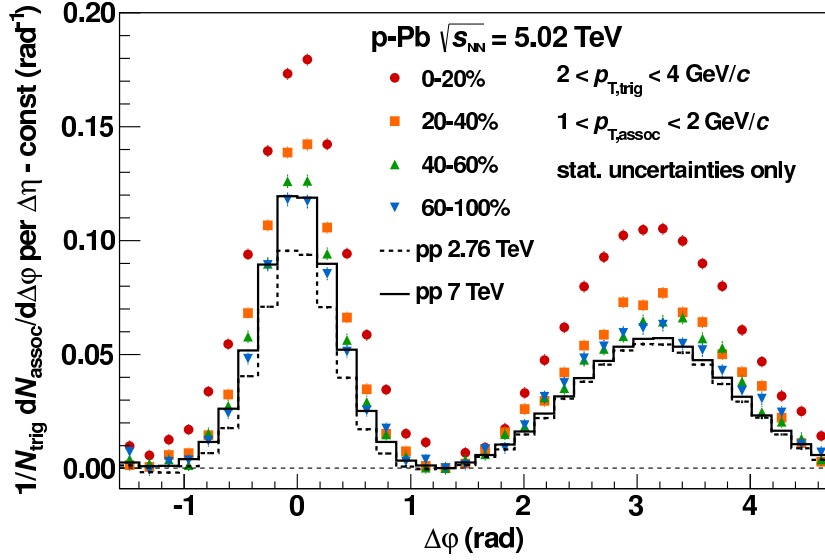


**Fig. 2:** Associated yield per trigger particle as a function of  $\Delta\phi$  averaged over  $|\Delta\eta| < 1.8$  for pairs of charged particles with  $2 < p_{T,\text{trig}} < 4 \text{ GeV}/c$  and  $1 < p_{T,\text{assoc}} < 2 \text{ GeV}/c$  in p–Pb collisions at  $\sqrt{s_{\text{NN}}} = 5.02 \text{ TeV}$  for different event classes, compared to pp collisions at 2.76 and 7 TeV. The yield between the peaks (determined at  $\Delta\phi \approx 1.3$ ) has been subtracted in each case. Only statistical uncertainties are shown; systematic uncertainties are less than 0.01 (absolute) per bin.

The top right panel in Fig. 3 shows the projection of Fig. 3 left to  $\Delta\eta$  averaged over different  $\Delta\phi$  intervals. The near-side and away-side distributions are flat apart from the discussed small peak around  $\Delta\eta = 0$ . The bottom right panel shows the projection to  $\Delta\phi$ , where a modulation is observed. For comparison, the subtracted associated yield for HIJING simulated events shifted to the baseline of the data is also shown, where no significant modulation remains. To quantify the near-side and away-side excess structures, the following functional form

$$1/N_{\text{trig}} dN_{\text{assoc}}/d\Delta\phi = a_0 + 2a_2 \cos(2\Delta\phi) + 2a_3 \cos(3\Delta\phi) \quad (2)$$

is fit to the data in multiplicity and  $p_T$  intervals. The fit has a  $\chi^2/\text{ndf}$  of 1–1.5 in the different  $p_T$  and multiplicity intervals, indicating that the data are well described by the fits. An example for the fit with and without the  $a_3 \cos(3\Delta\phi)$  term is shown in the bottom right panel of Fig. 3. The fit parameters  $a_2$  and  $a_3$  are a measure of the absolute modulation in the subtracted per-trigger yield and characterize a modulation relative to the baseline  $b$  in the higher multiplicity class assuming that such a modulation is not present in the 60–100% event class. This assumption has been checked by subtracting the yields obtained in  $\sqrt{s} = 2.76$  and 7 TeV pp collisions from the yields obtained for the 60–100% p–Pb event class and verifying that in both cases no significant signal remains. Therefore, the Fourier coefficients  $v_n$  of the corresponding single-particle distribution, commonly used in the analysis of particle correlations in nucleus–nucleus collisions [15], can be obtained in bins where the  $p_{T,\text{trig}}$  and  $p_{T,\text{assoc}}$  intervals are identical using

$$v_n = \sqrt{a_n/b}. \quad (3)$$

The baseline  $b$  is evaluated in the higher-multiplicity class in the region  $|\Delta\phi - \pi/2| < 0.2$ , corrected for the fact that it is obtained in the minimum of Eq. 2. A potential bias due to the above-mentioned incomplete near-side peak subtraction on  $v_2$  and  $v_3$  is evaluated in the following way: a) the size of the near-side exclusion region is changed from  $|\Delta\eta| < 0.8$  to

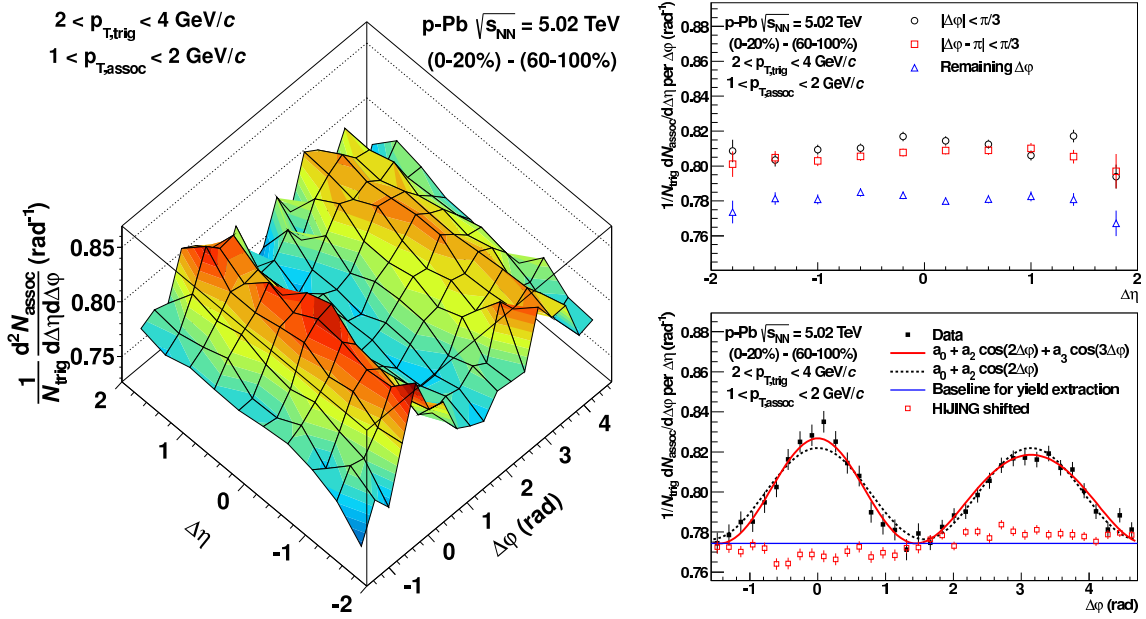


**Fig. 3:** Left: Associated yield per trigger particle in  $\Delta\phi$  and  $\Delta\eta$  for pairs of charged particles with  $2 < p_{T,\text{trig}} < 4 \text{ GeV}/c$  and  $1 < p_{T,\text{assoc}} < 2 \text{ GeV}/c$  in p–Pb collisions at  $\sqrt{s_{\text{NN}}} = 5.02 \text{ TeV}$  for the 0–20% multiplicity class, after subtraction of the associated yield obtained in the 60–100% event class. Top right: The associated per-trigger yield after subtraction (as shown on the left) projected onto  $\Delta\eta$  averaged over  $|\Delta\phi| < \pi/3$  (black circles),  $|\Delta\phi - \pi| < \pi/3$  (red squares), and the remaining area (blue triangles,  $\Delta\phi < -\pi/3$ ,  $\pi/3 < \Delta\phi < 2\pi/3$  and  $\Delta\phi > 4\pi/3$ ). Bottom right: as above but projected onto  $\Delta\phi$  averaged over  $0.8 < |\Delta\eta| < 1.8$  on the near side and  $|\Delta\eta| < 1.8$  on the away side. Superimposed are fits containing a  $\cos(2\Delta\phi)$  shape alone (black dashed line) and a combination of  $\cos(2\Delta\phi)$  and  $\cos(3\Delta\phi)$  shapes (red solid line). The blue horizontal line shows the baseline obtained from the latter fit which is used for the yield calculation. For comparison, the subtracted associated yield applying the same procedure on HIJING shifted to the same baseline is also shown. The figure shows only statistical uncertainties. Systematic uncertainties are mostly correlated and affect the baseline. Uncorrelated uncertainties are less than 1%.

$|\Delta\eta| < 1.2$ ; b) the residual near-side peak above the ridge is also removed from the away side accounting for the general  $p_T$ -dependent difference of near-side and away-side jet yields due to the kinematic constraints and the detector acceptance, which is evaluated using the lowest multiplicity class; and c) the lower multiplicity class is scaled before the subtraction such that no residual near-side peak above the ridge remains. The resulting differences in  $v_2$  (up to 15%) and  $v_3$  coefficients (up to 40%) when applying these approaches have been added to the systematic uncertainties.

The coefficients  $v_2$  and  $v_3$  are shown in the left panel of Fig. 4 for different event classes. The coefficient  $v_2$  increases with increasing  $p_T$ , and shows only a small dependence on multiplicity. In the 0–20% event class,  $v_2$  increases from  $0.06 \pm 0.01$  for  $0.5 < p_T < 1 \text{ GeV}/c$  to  $0.12 \pm 0.02$  for  $2 < p_T < 4 \text{ GeV}/c$ , while  $v_3$  is about 0.03 and shows, within large errors, an increasing trend with  $p_T$ . Reference [33] gives predictions for two-particle correlations arising from collective flow in p–Pb collisions at the LHC in the framework of a hydrodynamical model. The values for  $v_2$  and  $v_3$  coefficients, as well as the  $p_T$  and the multiplicity dependences, are in qualitative agreement with the presented results.



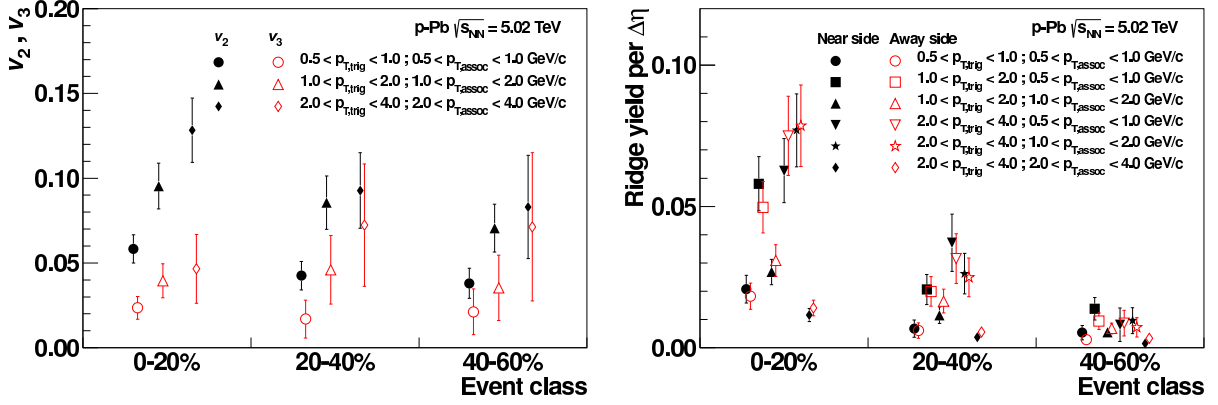


**Fig. 4:** Left:  $v_2$  (black closed symbols) and  $v_3$  (red open symbols) for different multiplicity classes and overlapping  $p_{T,assoc}$  and  $p_{T,trig}$  intervals. Right: Near-side (black closed symbols) and away-side (red open symbols) ridge yields per unit of  $\Delta\eta$  for different  $p_{T,trig}$  and  $p_{T,assoc}$  bins as a function of the multiplicity class. The error bars show statistical and systematic uncertainties added in quadrature. In both panels the points are slightly displaced horizontally for visibility.

To extract information on the yields and widths of the excess distributions in Fig. 3 (bottom right), a constant baseline assuming zero yield at the minimum of the fit function (Eq. 2) is subtracted. The remaining yield is integrated on the near side and on the away side. Alternatively, a baseline evaluated from the minimum of a parabolic function fitted within  $|\Delta\phi - \pi/2| < 1$  is used; the difference on the extracted yields is added to the systematic uncertainties. The uncertainty imposed by the residual near-side jet peak on the yield is evaluated in the same way as for the  $v_n$  coefficients. The near-side and away-side ridge yields are shown in the right panel of Fig. 4 for different event classes and for different combinations of  $p_{T,trig}$  and  $p_{T,assoc}$  intervals. The near-side and away-side yields range from 0 to 0.08 per unit of  $\Delta\eta$  depending on multiplicity class and  $p_T$  interval. It is remarkable that the near-side and away-side yields always agree within uncertainties for a given sample despite the fact that the absolute values change substantially with event class and  $p_T$  interval. Such a tight correlation between the yields is non-trivial and suggests a common underlying physical origin for the near-side and the away-side ridges.

From the baseline-subtracted per-trigger yields the square root of the variance,  $\sigma$ , within  $|\Delta\phi| < \pi/2$  and  $\pi/2 < \Delta\phi < 3\pi/2$  for the near-side and away-side region, respectively, is calculated. The extracted widths on the near side and the away side agree with each other within 20% and vary between 0.5 and 0.7. There is no significant  $p_T$  dependence suggesting that the observed ridge is not of jet origin.

The analysis has been repeated using the forward ZNA detector instead of the VZERO for the definition of the event classes. Unlike in nucleus–nucleus collisions, the correlation between forward energy measured in the ZNA and particle density at central rapidities is very weak in proton–nucleus collisions. Therefore, event classes defined as fixed fractions of the signal distribution in the ZNA select different events, with different mean particle multiplicity at midrapidity, than the samples selected with the same fractions in the VZERO detector. While the event classes selected with the ZNA span a much smaller range in central multiplicity density, they also minimize any autocorrelation between multiplicity selections and, for example, jet activity. With the ZNA selection, we find qualitatively consistent results compared to the VZERO selection, in particular an essentially symmetric excess correlation structure in the difference between low-multiplicity and high-multiplicity ZNA selected events, but also  $v_n$  coefficients

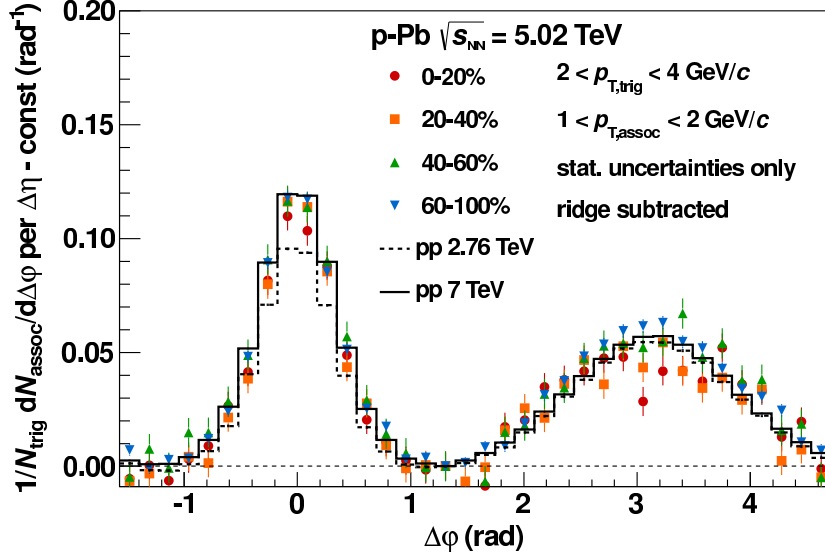


**Fig. 5:** Associated yield per trigger particle as a function of  $\Delta\phi$  averaged over  $|\Delta\eta| < 1.8$  for pairs of charged particles with  $2 < p_{T,\text{trig}} < 4 \text{ GeV}/c$  and  $1 < p_{T,\text{assoc}} < 2 \text{ GeV}/c$  in p–Pb collisions at  $\sqrt{s_{\text{NN}}} = 5.02 \text{ TeV}$  for different event classes, compared to pp collisions at  $\sqrt{s} = 2.76$  and  $7 \text{ TeV}$ . For the event classes 0–20%, 20–40% and 40–60% the long-range contribution on the near-side  $1.2 < |\Delta\eta| < 1.8$  and  $|\Delta\phi| < \pi/2$  has been subtracted from both the near side and the away side as described in the text. Subsequently, the yield between the peaks (determined at  $\Delta\phi \approx 1.3$ ) has been subtracted in each case. Only statistical uncertainties are shown; systematic uncertainties are less than 0.01 (absolute) per bin.

and  $\sigma$  widths which are similar within uncertainties. However, both the ridge yields and mean charged-particle multiplicity density at midrapidity are different between the VZERO and ZNA event classes. Nevertheless, within the uncertainties, both follow a common linear trend as a  
 275 function of  $\langle dN_{\text{ch}}/d\eta \rangle_{|\eta| < 0.5}$ .

So far it has been seen that the assumption of an unmodified jet shape in different multiplicity classes in p–Pb collisions resulted in the emergence of almost identical ridge-like excess structures on the near side and away side, most pronounced in high-multiplicity events. An alternative way is to start with the assumption that there are identical ridge structures on the  
 280 near side and away side, and to study whether this assumption leaves any room for multiplicity dependent modifications of the jet shape, in particular on the away side. To this end, a symmetric ridge structure is subtracted on near side and away side from the  $\Delta\phi$  projection of the associated yield per trigger averaged over  $|\Delta\eta| < 1.8$ . The near-side ridge structure is determined in the same event class within  $1.2 < |\Delta\eta| < 1.8$ , while the ridge on the away side  
 285 is constructed by mirroring this near-side structure at  $\Delta\phi = \pi/2$ . The ridge-subtracted results in the interval  $2 < p_{T,\text{trig}} < 4 \text{ GeV}/c$  and  $1 < p_{T,\text{assoc}} < 2 \text{ GeV}/c$  for the 0–20%, 20–40% and 40–60% event classes are shown in Fig. 5 compared to the unsubtracted 60–100% event class and to pp collisions. The remaining yields in all event classes are in agreement with each other and with pp collisions, indicating that the observed correlations are indeed consistent with a  
 290 symmetric ridge and with no further significant modification of the jet structure at midrapidity in high-multiplicity p–Pb collisions at the LHC, in contrast to what was seen at forward rapidity in  $\sqrt{s_{\text{NN}}} = 0.2 \text{ TeV}$  d–Au collisions at RHIC [35].

## 6 Summary

Results from angular correlations between charged trigger and associated particles in p–Pb collisions at  $\sqrt{s_{\text{NN}}} = 5.02$  TeV are presented for transverse momentum ranges within  $0.5 < p_{\text{T,assoc}} < p_{\text{T,trig}} < 4$  GeV/c. Associated yields per trigger particle are measured over two units of pseudorapidity and full azimuthal angle in different multiplicity classes. The yields projected onto  $\Delta\phi$  are increasing with event multiplicity and rise to values higher than those observed in pp collisions at  $\sqrt{s} = 2.76$  and 7 TeV. The difference between the yields per trigger particle in high-multiplicity and low-multiplicity events exhibits two long-range (up to  $|\Delta\eta| \sim 2$ ) ridge-like, nearly identical excess structures on the near-side ( $\Delta\phi \approx 0$ ) and away-side ( $\Delta\phi \approx \pi$ ) quantified by their yields and widths. The excess on the near side is qualitatively similar to the one recently reported by the CMS collaboration in  $2 < |\Delta\eta| < 4$  [22]. The excess on the away side is reported here for the first time. The event multiplicity and  $p_{\text{T}}$  dependences of the near-side and away-side ridge yields are in good agreement, while their width shows no significant dependence on multiplicity or  $p_{\text{T}}$ . The extracted  $v_2$  and  $v_3$  coefficients are in qualitative agreement with a hydrodynamical model calculation [34]. After subtracting the near-side ridge from the near side and away side symmetrically, the correlation shape in  $\Delta\phi$  becomes independent of multiplicity and similar to those of pp collisions at 7 TeV. There is no evidence for further significant structures in two-particle correlations at midrapidity in p–Pb collisions at  $\sqrt{s_{\text{NN}}} = 5.02$  TeV.

## Acknowledgements

The ALICE collaboration would like to thank all its engineers and technicians for their invaluable contributions to the construction of the experiment and the CERN accelerator teams for the outstanding performance of the LHC complex.

The ALICE collaboration acknowledges the following funding agencies for their support in building and running the ALICE detector:

State Committee of Science, Calouste Gulbenkian Foundation from Lisbon and Swiss Fonds Kidagan, Armenia;

Conselho Nacional de Desenvolvimento Científico e Tecnológico (CNPq), Financiadora de Estudos e Projetos (FINEP), Fundação de Amparo à Pesquisa do Estado de São Paulo (FAPESP);

National Natural Science Foundation of China (NSFC), the Chinese Ministry of Education (CMOE) and the Ministry of Science and Technology of China (MSTC);

Ministry of Education and Youth of the Czech Republic;

Danish Natural Science Research Council, the Carlsberg Foundation and the Danish National Research Foundation;

The European Research Council under the European Community’s Seventh Framework Programme;

Helsinki Institute of Physics and the Academy of Finland;

French CNRS-IN2P3, the ‘Region Pays de Loire’, ‘Region Alsace’, ‘Region Auvergne’ and CEA, France;

German BMBF and the Helmholtz Association;

General Secretariat for Research and Technology, Ministry of Development, Greece;

Hungarian OTKA and National Office for Research and Technology (NKTH);

Department of Atomic Energy and Department of Science and Technology of the Government

of India;  
 Istituto Nazionale di Fisica Nucleare (INFN) of Italy;  
 MEXT Grant-in-Aid for Specially Promoted Research, Japan;  
 340 Joint Institute for Nuclear Research, Dubna;  
 National Research Foundation of Korea (NRF);  
 CONACYT, DGAPA, México, ALFA-EC and the HELEN Program (High-Energy physics  
 Latin-American–European Network);  
 Stichting voor Fundamenteel Onderzoek der Materie (FOM) and the Nederlandse Organisatie  
 345 voor Wetenschappelijk Onderzoek (NWO), Netherlands;  
 Research Council of Norway (NFR);  
 Polish Ministry of Science and Higher Education;  
 National Authority for Scientific Research - NASR (Autoritatea Națională pentru Cercetare  
 Științifică - ANCS);  
 350 Ministry of Education and Science of Russian Federation, International Science and  
 Technology Center, Russian Academy of Sciences, Russian Federal Agency of Atomic  
 Energy, Russian Federal Agency for Science and Innovations and CERN-INTAS;  
 Ministry of Education of Slovakia;  
 Department of Science and Technology, South Africa;  
 355 CIEMAT, EELA, Ministerio de Educación y Ciencia of Spain, Xunta de Galicia (Consellería  
 de Educación), CEADEN, Cubaenergía, Cuba, and IAEA (International Atomic Energy  
 Agency);  
 Swedish Research Council (VR) and Knut & Alice Wallenberg Foundation (KAW);  
 Ukraine Ministry of Education and Science;  
 360 United Kingdom Science and Technology Facilities Council (STFC);  
 The United States Department of Energy, the United States National Science Foundation, the  
 State of Texas, and the State of Ohio.

## References

- [1] X.-N. Wang, “Studying mini - jets via the P(T) dependence of the two particle correlation  
 365 in azimuthal angle Phi,” *Phys.Rev.* **D47** (1993) 2754–2760, arXiv:hep-ph/9306215  
 [hep-ph].
- [2] **STAR** Collaboration, J. Adams *et al.*, “Minijet deformation and charge-independent  
 angular correlations on momentum subspace (eta, phi) in Au-Au collisions at  $\sqrt{s_{NN}} =$   
 130-GeV,” *Phys.Rev.* **C73** (2006) 064907, arXiv:nucl-ex/0411003 [nucl-ex].
- 370 [3] **PHOBOS** Collaboration, B. Alver *et al.*, “System size dependence of cluster properties  
 from two- particle angular correlations in Cu+Cu and Au+Au collisions at  $\sqrt{s_{NN}} = 200$   
 GeV,” *Phys.Rev.* **C81** (2010) 024904, arXiv:0812.1172 [nucl-ex].
- [4] **PHOBOS** Collaboration, B. Alver *et al.*, “High transverse momentum triggered  
 correlations over a large pseudorapidity acceptance in Au+Au collisions at  $\sqrt{s_{NN}} = 200$   
 375 GeV,” *Phys.Rev.Lett.* **104** (2010) 062301, arXiv:0903.2811 [nucl-ex].
- [5] **STAR** Collaboration, B. I. Abelev *et al.*, “Long range rapidity correlations and jet  
 production in high energy nuclear collisions,” *Phys.Rev.* **C80** (2009) 064912,  
 arXiv:0909.0191 [nucl-ex].

- [6] CMS Collaboration, S. Chatrchyan *et al.*, “Long-range and short-range dihadron angular correlations in central PbPb collisions at a nucleon-nucleon center of mass energy of 2.76 TeV,” *JHEP* **1107** (2011) 076, arXiv:1105.2438 [nucl-ex].
- [7] ALICE Collaboration, K. Aamodt *et al.*, “Harmonic decomposition of two-particle angular correlations in Pb–Pb collisions at  $\sqrt{s_{NN}} = 2.76$  TeV,” *Phys.Lett.* **B708** (2012) 249–264, arXiv:1109.2501 [nucl-ex].
- [8] STAR Collaboration, G. Agakishiev *et al.*, “Anomalous centrality evolution of two-particle angular correlations from Au-Au collisions at  $\sqrt{s_{NN}} = 62$  and 200 GeV,” arXiv:1109.4380 [nucl-ex].
- [9] CMS Collaboration, S. Chatrchyan *et al.*, “Centrality dependence of dihadron correlations and azimuthal anisotropy harmonics in PbPb collisions at  $\sqrt{s[NN]} = 2.76$  TeV,” *Eur.Phys.J.* **C72** (2012) 2012, arXiv:1201.3158 [nucl-ex].
- [10] ATLAS Collaboration, G. Aad *et al.*, “Measurement of the azimuthal anisotropy for charged particle production in  $\sqrt{s_{NN}} = 2.76$  TeV lead-lead collisions with the ATLAS detector,” *Phys.Rev.* **C86** (2012) 014907, arXiv:1203.3087 [hep-ex].
- [11] ALICE Collaboration, K. Aamodt *et al.*, “Higher harmonic anisotropic flow measurements of charged particles in Pb+Pb collisions at 2.76 TeV,” *Phys.Rev.Lett.* **107** no. 3, (Jul, 2011) 032301, arXiv:1105.3865 [nucl-ex].
- [12] PHENIX Collaboration, A. Adare *et al.*, “Measurements of higher-order flow harmonics in Au–Au collisions at  $\sqrt{s_{NN}} = 200$  GeV,” *Phys.Rev.Lett.* **107** (2011) 252301, arXiv:1105.3928 [nucl-ex].
- [13] ALICE Collaboration, B. Abelev *et al.*, “Anisotropic flow of charged hadrons, pions and (anti-)protons measured at high transverse momentum in Pb-Pb collisions at  $\sqrt{s_{NN}} = 2.76$  TeV,” arXiv:1205.5761 [nucl-ex].
- [14] CMS Collaboration, S. Chatrchyan *et al.*, “Measurement of the azimuthal anisotropy of neutral pions in PbPb collisions at  $\sqrt{s(NN)} = 2.76$  TeV,” arXiv:1208.2470 [nucl-ex].
- [15] S. Voloshin and Y. Zhang, “Flow study in relativistic nuclear collisions by Fourier expansion of Azimuthal particle distributions,” *Z.Phys.* **C70** (1996) 665–672, arXiv:hep-ph/9407282.
- [16] J.-Y. Ollitrault, “Anisotropy as a signature of transverse collective flow,” *Phys.Rev.* **D46** (1992) 229–245.
- [17] B. Alver and G. Roland, “Collision geometry fluctuations and triangular flow in heavy-ion collisions,” *Phys.Rev.* **C81** (2010) 054905, arXiv:1003.0194 [nucl-th].
- [18] B. Alver, C. Gombeaud, M. Luzum, and J.-Y. Ollitrault, “Triangular flow in hydrodynamics and transport theory,” *Phys.Rev.* **C82** (2010) 034913, arXiv:1007.5469 [nucl-th].

- [19] B. Schenke, S. Jeon, and C. Gale, “Elliptic and triangular flow in event-by-event (3+1)D viscous hydrodynamics,” *Phys.Rev.Lett.* **106** (2011) 042301, arXiv:1009.3244 [hep-ph].
- [20] Z. Qiu, C. Shen, and U. Heinz, “Hydrodynamic elliptic and triangular flow in Pb-Pb collisions at  $\sqrt{s} = 2.76$  ATeV,” *Phys.Lett.* **B707** (2012) 151–155, arXiv:1110.3033 [nucl-th].
- [21] CMS Collaboration, V. Khachatryan *et al.*, “Observation of Long-Range Near-Side Angular Correlations in Proton-Proton Collisions at the LHC,” *JHEP* **09** (2010) 091, arXiv:1009.4122 [hep-ex].
- [22] CMS Collaboration, S. Chatrchyan *et al.*, “Observation of long-range near-side angular correlations in proton-lead collisions at the LHC,” arXiv:1210.5482 [nucl-ex].
- [23] B. Arbusov, E. Boos, and V. Savrin, “CMS ridge effect at LHC as a manifestation of bremsstrahlung of gluons due to the quark-anti-quark string formation,” *Eur.Phys.J.* **C71** (2011) 1730, arXiv:1104.1283 [hep-ph].
- [24] K. Dusling and R. Venugopalan, “Evidence for BFKL and saturation dynamics from di-hadron spectra at the LHC,” arXiv:1210.3890 [hep-ph].
- [25] K. Dusling and R. Venugopalan, “Explanation of systematics of CMS p-Pb high multiplicity di-hadron data at  $\sqrt{s_{NN}} = 5.02$  TeV,” arXiv:1211.3701 [hep-ph].
- [26] C.-Y. Wong, “Momentum kick model description of the ridge in  $\Delta\phi$ - $\Delta\eta$  correlation in pp collisions at 7 TeV,” *Phys.Rev.* **C84** (2011) 024901, arXiv:1105.5871 [hep-ph].
- [27] M. Strikman, “Transverse nucleon structure and multiparton interactions,” *Acta Phys.Polon.* **B42** (2011) 2607–2630, arXiv:1112.3834 [hep-ph].
- [28] S. Alderweireldt and P. Van Mechelen, “Obtaining the CMS Ridge effect with multiparton interactions,” arXiv:1203.2048 [hep-ph].
- [29] E. Avsar, C. Flensburg, Y. Hatta, J.-Y. Ollitrault, and T. Ueda, “Eccentricity and elliptic flow in proton-proton collisions from parton evolution,” *Phys.Lett.* **B702** (2011) 394–397, arXiv:1009.5643 [hep-ph].
- [30] K. Werner, I. Karpenko, and T. Pierog, “The ‘ridge’ in pp scattering at 7 TeV,” *Phys.Rev.Lett.* **106** (2011) 122004, arXiv:1011.0375 [hep-ph].
- [31] W.-T. Deng, Z. Xu, and C. Greiner, “Elliptic and triangular flow and their correlation in ultrarelativistic high multiplicity pp collisions at 14 TeV,” *Phys.Lett.* **B711** (2012) 301–306, arXiv:1112.0470 [hep-ph].
- [32] E. Avsar, Y. Hatta, C. Flensburg, J. Ollitrault, and T. Ueda, “Eccentricity and elliptic flow in pp collisions at the LHC,” *J.Phys.* **G38** (2011) 124053, arXiv:1106.4356 [hep-ph].
- [33] P. Bozek, “Collective flow in p-Pb and d-Pb collisions at TeV energies,” *Phys.Rev.* **C85** (2012) 014911, arXiv:1112.0915 [hep-ph].

- [34] P. Bozek and W. Broniowski, “Correlations from hydrodynamic flow in p-Pb collisions,” arXiv:1211.0845 [nucl-th].
- [35] **STAR** Collaboration, E. Braidot, “Suppression of forward pion correlations in d–Au interactions at STAR,” arXiv:1005.2378 [hep-ph].
- [36] J. L. Albacete and C. Marquet, “Azimuthal correlations of forward di-hadrons in d+Au collisions at RHIC in the Color Glass Condensate,” *Phys.Rev.Lett.* **105** (2010) 162301, arXiv:1005.4065 [hep-ph].
- [37] **ALICE** Collaboration, K. Aamodt *et al.*, “The ALICE experiment at the CERN LHC,” *JINST* **3** (2008) S08002.
- [38] **ALICE** Collaboration, K. Aamodt *et al.*, “Charged-particle multiplicity measurement in proton-proton collisions at  $\sqrt{s} = 0.9$  and 2.36 TeV with ALICE at LHC,” *Eur.Phys.J.* **C68** (2010) 89–108, arXiv:1004.3034 [hep-ex].
- [39] **ALICE** Collaboration, B. Abelev *et al.*, “Pseudorapidity density of charged particles p–Pb collisions at  $\sqrt{s_{NN}} = 5.02$  TeV,” arXiv:1210.3615 [nucl-ex].
- [40] **ALICE** Collaboration, B. Abelev *et al.*, “Centrality dependence of charged particle production at large transverse momentum in Pb–Pb collisions at  $\sqrt{s_{NN}} = 2.76$  TeV,” arXiv:1208.2711 [hep-ex].
- [41] **ALICE** Collaboration, B. Abelev *et al.*, “Measurement of event background fluctuations for charged particle jet reconstruction in Pb–Pb collisions at  $\sqrt{s_{NN}} = 2.76$  TeV,” *JHEP* **1203** (2012) 053, arXiv:1201.2423 [hep-ex].
- [42] **ALICE** Collaboration, B. Abelev *et al.*, “Underlying event measurements in pp collisions at  $\sqrt{s} = 0.9$  and 7 TeV with the ALICE experiment at the LHC,” *JHEP* **1207** (2012) 116, arXiv:1112.2082 [hep-ex].
- [43] S. Roesler, R. Engel, and J. Ranft, “The Monte Carlo event generator DPMJET-III,” arXiv:hep-ph/0012252.
- [44] T. Sjostrand, S. Mrenna, and P. Z. Skands, “PYTHIA 6.4 physics and manual,” *JHEP* **0605** (2006) 026, arXiv:hep-ph/0603175 [hep-ph].
- [45] P. Z. Skands, “Tuning Monte Carlo generators: The Perugia tunes,” *Phys.Rev.* **D82** (2010) 074018, arXiv:1005.3457 [hep-ph].
- [46] R. Brun *et al.*, “Geant detector description and simulation tool,” *CERN Program Library Long Write-up*, W5013 (1994).
- [47] X.-N. Wang and M. Gyulassy, “HIJING: A Monte Carlo model for multiple jet production in pp, pA and AA collisions,” *Phys.Rev.* **D44** (1991) 3501.

485 **A The ALICE Collaboration**

B. Abelev<sup>71</sup>, J. Adam<sup>37</sup>, D. Adamová<sup>78</sup>, A.M. Adare<sup>127</sup>, M.M. Aggarwal<sup>82</sup>, G. Aglieri Rinella<sup>33</sup>, M. Agnello<sup>102,88</sup>, A.G. Agocs<sup>126</sup>, A. Agostinelli<sup>27</sup>, Z. Ahammed<sup>122</sup>, N. Ahmad<sup>17</sup>, A. Ahmad Masoodi<sup>17</sup>, S.A. Ahn<sup>64</sup>, S.U. Ahn<sup>40,64</sup>, M. Ajaz<sup>15</sup>, A. Akindinov<sup>50</sup>, D. Aleksandrov<sup>94</sup>, B. Alessandro<sup>102</sup>, A. Alici<sup>98,12</sup>, A. Alkin<sup>3</sup>, E. Almaráz Aviña<sup>60</sup>, J. Alme<sup>35</sup>, T. Alt<sup>39</sup>, V. Altini<sup>31</sup>,  
490 S. Altinpinar<sup>18</sup>, I. Altsybeev<sup>123</sup>, C. Andrei<sup>74</sup>, A. Andronic<sup>91</sup>, V. Anguelov<sup>87</sup>, J. Anielski<sup>58</sup>, C. Anson<sup>19</sup>, T. Antičić<sup>92</sup>, F. Antinori<sup>99</sup>, P. Antonioli<sup>98</sup>, L. Aphecetche<sup>107</sup>, H. Appelshäuser<sup>56</sup>, N. Arbor<sup>67</sup>, S. Arcelli<sup>27</sup>, A. Arend<sup>56</sup>, N. Armesto<sup>16</sup>, R. Arnaldi<sup>102</sup>, T. Aronsson<sup>127</sup>, I.C. Arsene<sup>91</sup>, M. Arslandok<sup>56</sup>, A. Asryan<sup>123</sup>, A. Augustinus<sup>33</sup>, R. Averbeck<sup>91</sup>, T.C. Awes<sup>79</sup>, J. Äystö<sup>42</sup>, M.D. Azmi<sup>17,84</sup>, M. Bach<sup>39</sup>, A. Badalà<sup>105</sup>, Y.W. Baek<sup>66,40</sup>, R. Bailhache<sup>56</sup>, R. Bala<sup>85,102</sup>,  
495 R. Baldini Ferroli<sup>12</sup>, A. Baldisseri<sup>14</sup>, F. Baltasar Dos Santos Pedrosa<sup>33</sup>, J. Bán<sup>51</sup>, R.C. Baral<sup>52</sup>, R. Barbera<sup>26</sup>, F. Barile<sup>31</sup>, G.G. Barnaföldi<sup>126</sup>, L.S. Barnby<sup>96</sup>, V. Barret<sup>66</sup>, J. Bartke<sup>110</sup>, M. Basile<sup>27</sup>, N. Bastid<sup>66</sup>, S. Basu<sup>122</sup>, B. Bathen<sup>58</sup>, G. Batigne<sup>107</sup>, B. Batyunya<sup>62</sup>, C. Baumann<sup>56</sup>, I.G. Bearden<sup>76</sup>, H. Beck<sup>56</sup>, N.K. Behera<sup>44</sup>, I. Belikov<sup>61</sup>, F. Bellini<sup>27</sup>, R. Bellwied<sup>116</sup>, E. Belmont-Moreno<sup>60</sup>, G. Bencedi<sup>126</sup>, S. Beole<sup>22</sup>, I. Berceau<sup>74</sup>, A. Bercuci<sup>74</sup>, Y. Berdnikov<sup>80</sup>, D. Berenyi<sup>126</sup>,  
500 A.A.E. Bergognon<sup>107</sup>, D. Berzano<sup>22,102</sup>, L. Betev<sup>33</sup>, A. Bhasin<sup>85</sup>, A.K. Bhati<sup>82</sup>, J. Bhom<sup>120</sup>, L. Bianchi<sup>22</sup>, N. Bianchi<sup>68</sup>, J. Bielčák<sup>37</sup>, J. Bielčáková<sup>78</sup>, A. Bilandzic<sup>76</sup>, S. Bjelogrić<sup>49</sup>, F. Blanco<sup>116</sup>, F. Blanco<sup>10</sup>, D. Blau<sup>94</sup>, C. Blume<sup>56</sup>, M. Boccioni<sup>33</sup>, S. Böttger<sup>55</sup>, A. Bogdanov<sup>72</sup>, H. Bøggild<sup>76</sup>, M. Bogolyubsky<sup>47</sup>, L. Boldizsár<sup>126</sup>, M. Bombara<sup>38</sup>, J. Book<sup>56</sup>, H. Borel<sup>14</sup>, A. Borissov<sup>125</sup>, F. Bossú<sup>84</sup>, M. Botje<sup>77</sup>, E. Botta<sup>22</sup>, E. Braidot<sup>70</sup>, P. Braun-Munzinger<sup>91</sup>,  
505 M. Bregant<sup>107</sup>, T. Breitner<sup>55</sup>, T.A. Broker<sup>56</sup>, T.A. Browning<sup>89</sup>, M. Broz<sup>36</sup>, R. Brun<sup>33</sup>, E. Bruna<sup>22,102</sup>, G.E. Bruno<sup>31</sup>, D. Budnikov<sup>93</sup>, H. Buesching<sup>56</sup>, S. Bufalino<sup>22,102</sup>, P. Buncic<sup>33</sup>, O. Busch<sup>87</sup>, Z. Buthelezi<sup>84</sup>, D. Caballero Orduna<sup>127</sup>, D. Caffarri<sup>28,99</sup>, X. Cai<sup>7</sup>, H. Caines<sup>127</sup>, E. Calvo Villar<sup>97</sup>, P. Camerini<sup>24</sup>, V. Canoa Roman<sup>11</sup>, G. Cara Romeo<sup>98</sup>, W. Carena<sup>33</sup>, F. Carena<sup>33</sup>, N. Carlin Filho<sup>113</sup>, F. Carminati<sup>33</sup>, A. Casanova Díaz<sup>68</sup>, J. Castillo Castellanos<sup>14</sup>, J.F. Castillo Hernandez<sup>91</sup>,  
510 E.A.R. Casula<sup>23</sup>, V. Catanescu<sup>74</sup>, C. Cavicchioli<sup>33</sup>, C. Ceballos Sanchez<sup>9</sup>, J. Cepila<sup>37</sup>, P. Cerello<sup>102</sup>, B. Chang<sup>42,129</sup>, S. Chapeland<sup>33</sup>, J.L. Charvet<sup>14</sup>, S. Chattopadhyay<sup>95</sup>, S. Chattopadhyay<sup>122</sup>, I. Chawla<sup>82</sup>, M. Cherney<sup>81</sup>, C. Cheshkov<sup>33,115</sup>, B. Cheynis<sup>115</sup>, V. Chibante Barroso<sup>33</sup>, D.D. Chinellato<sup>116</sup>, P. Chochula<sup>33</sup>, M. Chojnacki<sup>76,49</sup>, S. Choudhury<sup>122</sup>, P. Christakoglou<sup>77</sup>, C.H. Christensen<sup>76</sup>, P. Christiansen<sup>32</sup>, T. Chujo<sup>120</sup>, S.U. Chung<sup>90</sup>, C. Cicalo<sup>101</sup>, L. Cifarelli<sup>27,33,12</sup>,  
515 F. Cindolo<sup>98</sup>, J. Cleymans<sup>84</sup>, F. Coccetti<sup>12</sup>, F. Colamaria<sup>31</sup>, D. Colella<sup>31</sup>, A. Collu<sup>23</sup>, G. Conesa Balbastre<sup>67</sup>, Z. Conesa del Valle<sup>33</sup>, M.E. Connors<sup>127</sup>, G. Contin<sup>24</sup>, J.G. Contreras<sup>11</sup>, T.M. Cormier<sup>125</sup>, Y. Corrales Morales<sup>22</sup>, P. Cortese<sup>30</sup>, I. Cortés Maldonado<sup>2</sup>, M.R. Cosentino<sup>70</sup>, F. Costa<sup>33</sup>, M.E. Cotallo<sup>10</sup>, E. Crescio<sup>11</sup>, P. Crochet<sup>66</sup>, E. Cruz Alaniz<sup>60</sup>, R. Cruz Albino<sup>11</sup>, E. Cuautle<sup>59</sup>, L. Cunqueiro<sup>68</sup>, A. Dainese<sup>28,99</sup>, H.H. Dalsgaard<sup>76</sup>, A. Danu<sup>54</sup>, I. Das<sup>46</sup>, D. Das<sup>95</sup>,  
520 S. Das<sup>4</sup>, K. Das<sup>95</sup>, A. Dash<sup>114</sup>, S. Dash<sup>44</sup>, S. De<sup>122</sup>, G.O.V. de Barros<sup>113</sup>, A. De Caro<sup>29,12</sup>, G. de Cataldo<sup>104</sup>, J. de Cuveland<sup>39</sup>, A. De Falco<sup>23</sup>, D. De Gruttola<sup>29</sup>, H. Delagrange<sup>107</sup>, A. Deloff<sup>73</sup>, N. De Marco<sup>102</sup>, E. Dénes<sup>126</sup>, S. De Pasquale<sup>29</sup>, A. Deppman<sup>113</sup>, G. D Eraso<sup>31</sup>, R. de Rooij<sup>49</sup>, M.A. Diaz Corchero<sup>10</sup>, D. Di Bari<sup>31</sup>, T. Dietel<sup>58</sup>, C. Di Giglio<sup>31</sup>, S. Di Liberto<sup>100</sup>, A. Di Mauro<sup>33</sup>, P. Di Nezza<sup>68</sup>, R. Divià<sup>33</sup>, Ø. Djuvsland<sup>18</sup>, A. Dobrin<sup>125,32</sup>, T. Dobrowolski<sup>73</sup>, B. Dönigus<sup>91</sup>,  
525 O. Dordic<sup>21</sup>, O. Driga<sup>107</sup>, A.K. Dubey<sup>122</sup>, A. Dubla<sup>49</sup>, L. Ducroux<sup>115</sup>, P. Dupieux<sup>66</sup>, A.K. Dutta Majumdar<sup>95</sup>, D. Elia<sup>104</sup>, D. Emschermann<sup>58</sup>, H. Engel<sup>55</sup>, B. Erazmus<sup>33,107</sup>, H.A. Erdal<sup>35</sup>, B. Espagnon<sup>46</sup>, M. Estienne<sup>107</sup>, S. Esumi<sup>120</sup>, D. Evans<sup>96</sup>, G. Eyyubova<sup>21</sup>, D. Fabris<sup>28,99</sup>, J. Faivre<sup>67</sup>, D. Falchieri<sup>27</sup>, A. Fantoni<sup>68</sup>, M. Fasel<sup>91,87</sup>, R. Fearick<sup>84</sup>, D. Fehlker<sup>18</sup>, L. Feldkamp<sup>58</sup>, D. Felea<sup>54</sup>, A. Feliciello<sup>102</sup>, B. Fenton-Olsen<sup>70</sup>, G. Feofilov<sup>123</sup>, A. Fernández Téllez<sup>2</sup>, A. Ferretti<sup>22</sup>,  
530 A. Festanti<sup>28</sup>, J. Figiel<sup>110</sup>, M.A.S. Figueredo<sup>113</sup>, S. Filchagin<sup>93</sup>, D. Finogeev<sup>48</sup>, F.M. Fionda<sup>31</sup>, E.M. Fiore<sup>31</sup>, E. Floratos<sup>83</sup>, M. Floris<sup>33</sup>, S. Foertsch<sup>84</sup>, P. Foka<sup>91</sup>, S. Fokin<sup>94</sup>, E. Fragiaco<sup>103</sup>, A. Francescon<sup>33,28</sup>, U. Frankfeld<sup>91</sup>, U. Fuchs<sup>33</sup>, C. Furgel<sup>67</sup>, M. Fusco Girard<sup>29</sup>, J.J. Gaardhøje<sup>76</sup>, M. Gagliardi<sup>22</sup>, A. Gago<sup>97</sup>, M. Gallio<sup>22</sup>, D.R. Gangadharan<sup>19</sup>, P. Ganoti<sup>79</sup>, C. Garabatos<sup>91</sup>,



E. Garcia-Solis<sup>13</sup>, I. Garishvili<sup>71</sup>, J. Gerhard<sup>39</sup>, M. Germain<sup>107</sup>, C. Geuna<sup>14</sup>, M. Gheata<sup>54,33</sup>,  
 535 A. Gheata<sup>33</sup>, B. Ghidini<sup>31</sup>, P. Ghosh<sup>122</sup>, P. Gianotti<sup>68</sup>, M.R. Girard<sup>124</sup>, P. Giubellino<sup>33</sup>,  
 E. Gladysz-Dziadus<sup>110</sup>, P. Glässel<sup>87</sup>, R. Gomez<sup>112,11</sup>, E.G. Ferreira<sup>16</sup>, L.H. González-Trueba<sup>60</sup>,  
 P. González-Zamora<sup>10</sup>, S. Gorbunov<sup>39</sup>, A. Goswami<sup>86</sup>, S. Gotovac<sup>109</sup>, L.K. Graczykowski<sup>124</sup>,  
 R. Grajcarek<sup>87</sup>, A. Grelli<sup>49</sup>, C. Grigoras<sup>33</sup>, A. Grigoras<sup>33</sup>, V. Grigoriev<sup>72</sup>, A. Grigoryan<sup>1</sup>,  
 S. Grigoryan<sup>62</sup>, B. Grinyov<sup>3</sup>, N. Grion<sup>103</sup>, P. Gros<sup>32</sup>, J.F. Grosse-Oetringhaus<sup>33</sup>, J.-Y. Grossiord<sup>115</sup>,  
 540 R. Grosso<sup>33</sup>, F. Guber<sup>48</sup>, R. Guernane<sup>67</sup>, B. Guerzoni<sup>27</sup>, M. Guilbaud<sup>115</sup>, K. Gulbrandsen<sup>76</sup>,  
 H. Gulkanyan<sup>1</sup>, T. Gunji<sup>119</sup>, A. Gupta<sup>85</sup>, R. Gupta<sup>85</sup>, R. Haake<sup>58</sup>, Ø. Haaland<sup>18</sup>, C. Hadjidakis<sup>46</sup>,  
 M. Haiduc<sup>54</sup>, H. Hamagaki<sup>119</sup>, G. Hamar<sup>126</sup>, B.H. Han<sup>20</sup>, L.D. Hanratty<sup>96</sup>, A. Hansen<sup>76</sup>,  
 Z. Harmanová-Tóthová<sup>38</sup>, J.W. Harris<sup>127</sup>, M. Hartig<sup>56</sup>, A. Harton<sup>13</sup>, D. Hatzifotiadou<sup>98</sup>,  
 S. Hayashi<sup>119</sup>, A. Hayrapetyan<sup>33,1</sup>, S.T. Heckel<sup>56</sup>, M. Heide<sup>58</sup>, H. Helstrup<sup>35</sup>, A. Herghelegiu<sup>74</sup>,  
 545 G. Herrera Corral<sup>11</sup>, N. Herrmann<sup>87</sup>, B.A. Hess<sup>121</sup>, K.F. Hetland<sup>35</sup>, B. Hicks<sup>127</sup>, B. Hippolyte<sup>61</sup>,  
 Y. Hori<sup>119</sup>, P. Hristov<sup>33</sup>, I. Hřivnáčová<sup>46</sup>, M. Huang<sup>18</sup>, T.J. Humanic<sup>19</sup>, D.S. Hwang<sup>20</sup>, R. Ichou<sup>66</sup>,  
 R. Ilkaev<sup>93</sup>, I. Ilkiv<sup>73</sup>, M. Inaba<sup>120</sup>, E. Incani<sup>23</sup>, P.G. Innocenti<sup>33</sup>, G.M. Innocenti<sup>22</sup>, M. Ippolitov<sup>94</sup>,  
 M. Irfan<sup>17</sup>, C. Ivan<sup>91</sup>, V. Ivanov<sup>80</sup>, A. Ivanov<sup>123</sup>, M. Ivanov<sup>91</sup>, O. Ivanytskyi<sup>3</sup>, A. Jacholkowski<sup>26</sup>,  
 P. M. Jacobs<sup>70</sup>, H.J. Jang<sup>64</sup>, M.A. Janik<sup>124</sup>, R. Janik<sup>36</sup>, P.H.S.Y. Jayarathna<sup>116</sup>, S. Jena<sup>44</sup>,  
 550 D.M. Jha<sup>125</sup>, R.T. Jimenez Bustamante<sup>59</sup>, P.G. Jones<sup>96</sup>, H. Jung<sup>40</sup>, A. Jusko<sup>96</sup>, A.B. Kaidalov<sup>50</sup>,  
 S. Kalcher<sup>39</sup>, P. Kaliňák<sup>51</sup>, T. Kalliokoski<sup>42</sup>, A. Kalweit<sup>57,33</sup>, J.H. Kang<sup>129</sup>, V. Kaplin<sup>72</sup>,  
 A. Karasu Uysal<sup>33,128,65</sup>, O. Karavichev<sup>48</sup>, T. Karavicheva<sup>48</sup>, E. Karpechev<sup>48</sup>, A. Kazantsev<sup>94</sup>,  
 U. Kebschull<sup>55</sup>, R. Keidel<sup>130</sup>, P. Khan<sup>95</sup>, S.A. Khan<sup>122</sup>, M.M. Khan<sup>17</sup>, K. H. Khan<sup>15</sup>,  
 A. Khanzadeev<sup>80</sup>, Y. Kharlov<sup>47</sup>, B. Kileng<sup>35</sup>, B. Kim<sup>129</sup>, J.S. Kim<sup>40</sup>, J.H. Kim<sup>20</sup>, D.J. Kim<sup>42</sup>,  
 555 D.W. Kim<sup>40,64</sup>, T. Kim<sup>129</sup>, S. Kim<sup>20</sup>, M. Kim<sup>40</sup>, M. Kim<sup>129</sup>, S. Kirsch<sup>39</sup>, I. Kisel<sup>39</sup>, S. Kiselev<sup>50</sup>,  
 A. Kisiel<sup>124</sup>, J.L. Klay<sup>6</sup>, J. Klein<sup>87</sup>, C. Klein-Bösing<sup>58</sup>, M. Kliemant<sup>56</sup>, A. Kluge<sup>33</sup>, M.L. Knichel<sup>91</sup>,  
 A.G. Knospe<sup>111</sup>, M.K. Köhler<sup>91</sup>, T. Kollegger<sup>39</sup>, A. Kolojvari<sup>123</sup>, M. Kompaniets<sup>123</sup>,  
 V. Kondratiev<sup>123</sup>, N. Kondratyeva<sup>72</sup>, A. Konevskikh<sup>48</sup>, V. Kovalenko<sup>123</sup>, M. Kowalski<sup>110</sup>, S. Kox<sup>67</sup>,  
 G. Koyithatta Meethalevedu<sup>44</sup>, J. Kral<sup>42</sup>, I. Králik<sup>51</sup>, F. Kramer<sup>56</sup>, A. Kravčáková<sup>38</sup>,  
 560 T. Krawutschke<sup>87,34</sup>, M. Krelina<sup>37</sup>, M. Kretz<sup>39</sup>, M. Krivda<sup>96,51</sup>, F. Krizek<sup>42</sup>, M. Krus<sup>37</sup>,  
 E. Kryshen<sup>80</sup>, M. Krzewicki<sup>91</sup>, Y. Kucheriaev<sup>94</sup>, T. Kugathasan<sup>33</sup>, C. Kuhn<sup>61</sup>, P.G. Kuijter<sup>77</sup>,  
 I. Kulakov<sup>56</sup>, J. Kumar<sup>44</sup>, P. Kurashvili<sup>73</sup>, A. Kurepin<sup>48</sup>, A.B. Kurepin<sup>48</sup>, A. Kuryakin<sup>93</sup>,  
 S. Kushpil<sup>78</sup>, V. Kushpil<sup>78</sup>, H. Kvaerno<sup>21</sup>, M.J. Kweon<sup>87</sup>, Y. Kwon<sup>129</sup>, P. Ladrón de Guevara<sup>59</sup>,  
 I. Lakomov<sup>46</sup>, R. Langoy<sup>18</sup>, S.L. La Pointe<sup>49</sup>, C. Lara<sup>55</sup>, A. Lardeux<sup>107</sup>, P. La Rocca<sup>26</sup>, R. Lea<sup>24</sup>,  
 565 M. Lechman<sup>33</sup>, K.S. Lee<sup>40</sup>, S.C. Lee<sup>40</sup>, G.R. Lee<sup>96</sup>, I. Legrand<sup>33</sup>, J. Lehnert<sup>56</sup>, M. Lenhardt<sup>91</sup>,  
 V. Lenti<sup>104</sup>, H. León<sup>60</sup>, I. León Monzón<sup>112</sup>, H. León Vargas<sup>56</sup>, P. Lévai<sup>126</sup>, S. Li<sup>7</sup>, J. Lien<sup>18</sup>,  
 R. Lietava<sup>96</sup>, S. Lindal<sup>21</sup>, V. Lindenstruth<sup>39</sup>, C. Lippmann<sup>91,33</sup>, M.A. Lisa<sup>19</sup>, H.M. Ljunggren<sup>32</sup>,  
 P.I. Loenne<sup>18</sup>, V.R. Loggins<sup>125</sup>, V. Loginov<sup>72</sup>, D. Lohner<sup>87</sup>, C. Loizides<sup>70</sup>, K.K. Loo<sup>42</sup>, X. Lopez<sup>66</sup>,  
 E. López Torres<sup>9</sup>, G. Løvhøiden<sup>21</sup>, X.-G. Lu<sup>87</sup>, P. Luettig<sup>56</sup>, M. Lunardon<sup>28</sup>, J. Luo<sup>7</sup>, G. Luparello<sup>49</sup>,  
 570 C. Luzzi<sup>33</sup>, R. Ma<sup>127</sup>, K. Ma<sup>7</sup>, D.M. Madagodahettige-Don<sup>116</sup>, A. Maevskaya<sup>48</sup>, M. Mager<sup>57,33</sup>,  
 D.P. Mahapatra<sup>52</sup>, A. Maire<sup>87</sup>, M. Malaev<sup>80</sup>, I. Maldonado Cervantes<sup>59</sup>, L. Malinina<sup>62,ii</sup>,  
 D. Mal'Kevich<sup>50</sup>, P. Malzacher<sup>91</sup>, A. Mamonov<sup>93</sup>, L. Manceau<sup>102</sup>, L. Mangotra<sup>85</sup>, V. Manko<sup>94</sup>,  
 F. Manso<sup>66</sup>, V. Manzari<sup>104</sup>, Y. Mao<sup>7</sup>, M. Marchisone<sup>66,22</sup>, J. Mares<sup>53</sup>, G.V. Margagliotti<sup>24,103</sup>,  
 A. Margotti<sup>98</sup>, A. Marín<sup>91</sup>, C. Markert<sup>111</sup>, M. Marquard<sup>56</sup>, I. Martashvili<sup>118</sup>, N.A. Martin<sup>91</sup>,  
 575 P. Martinengo<sup>33</sup>, M.I. Martínez<sup>2</sup>, A. Martínez Davalos<sup>60</sup>, G. Martínez García<sup>107</sup>, Y. Martynov<sup>3</sup>,  
 A. Mas<sup>107</sup>, S. Masciocchi<sup>91</sup>, M. Masera<sup>22</sup>, A. Masoni<sup>101</sup>, L. Massacrier<sup>107</sup>, A. Mastroserio<sup>31</sup>,  
 A. Matyja<sup>110,107</sup>, C. Mayer<sup>110</sup>, J. Mazer<sup>118</sup>, M.A. Mazzoni<sup>100</sup>, F. Meddi<sup>25</sup>, A. Menchaca-Rocha<sup>60</sup>,  
 J. Mercado Pérez<sup>87</sup>, M. Meres<sup>36</sup>, Y. Miake<sup>120</sup>, L. Milano<sup>22</sup>, J. Milosevic<sup>21,iii</sup>, A. Mischke<sup>49</sup>,  
 A.N. Mishra<sup>86,45</sup>, D. Miśkowiec<sup>91</sup>, C. Mitu<sup>54</sup>, S. Mizuno<sup>120</sup>, J. Mlynarz<sup>125</sup>, B. Mohanty<sup>122,75</sup>,  
 580 L. Molnar<sup>126,33,61</sup>, L. Montaña Zetina<sup>11</sup>, M. Monteno<sup>102</sup>, E. Montes<sup>10</sup>, T. Moon<sup>129</sup>, M. Morando<sup>28</sup>,  
 D.A. Moreira De Godoy<sup>113</sup>, S. Moretto<sup>28</sup>, A. Morreale<sup>42</sup>, A. Morsch<sup>33</sup>, V. Muccifora<sup>68</sup>,  
 E. Mudnic<sup>109</sup>, S. Muhuri<sup>122</sup>, M. Mukherjee<sup>122</sup>, H. Müller<sup>33</sup>, M.G. Munhoz<sup>113</sup>, S. Murray<sup>84</sup>,  
 L. Musa<sup>33</sup>, J. Musinsky<sup>51</sup>, A. Musso<sup>102</sup>, B.K. Nandi<sup>44</sup>, R. Nania<sup>98</sup>, E. Nappi<sup>104</sup>, C. Nattrass<sup>118</sup>,

T.K. Nayak<sup>122</sup>, S. Nazarenko<sup>93</sup>, A. Nedosekin<sup>50</sup>, M. Nicassio<sup>31,91</sup>, M. Niculescu<sup>54,33</sup>,  
585 B.S. Nielsen<sup>76</sup>, T. Niida<sup>120</sup>, S. Nikolaev<sup>94</sup>, V. Nikolic<sup>92</sup>, S. Nikulin<sup>94</sup>, V. Nikulin<sup>80</sup>, B.S. Nilsen<sup>81</sup>,  
M.S. Nilsson<sup>21</sup>, F. Noferini<sup>98,12</sup>, P. Nomokonov<sup>62</sup>, G. Nooren<sup>49</sup>, N. Novitzky<sup>42</sup>, A. Nyanin<sup>94</sup>,  
A. Nyatha<sup>44</sup>, C. Nygaard<sup>76</sup>, J. Nystrand<sup>18</sup>, A. Ochirov<sup>123</sup>, H. Oeschler<sup>57,33</sup>, S. Oh<sup>127</sup>, S.K. Oh<sup>40</sup>,  
J. Oleniacz<sup>124</sup>, A.C. Oliveira Da Silva<sup>113</sup>, C. Oppedisano<sup>102</sup>, A. Ortiz Velasquez<sup>32,59</sup>,  
A. Oskarsson<sup>32</sup>, P. Ostrowski<sup>124</sup>, J. Otwinowski<sup>91</sup>, K. Oyama<sup>87</sup>, K. Ozawa<sup>119</sup>, Y. Pachmayer<sup>87</sup>,  
590 M. Pachr<sup>37</sup>, F. Padilla<sup>22</sup>, P. Pagano<sup>29</sup>, G. Paic<sup>59</sup>, F. Painke<sup>39</sup>, C. Pajares<sup>16</sup>, S.K. Pal<sup>122</sup>, A. Palaha<sup>96</sup>,  
A. Palmeri<sup>105</sup>, V. Papikyan<sup>1</sup>, G.S. Pappalardo<sup>105</sup>, W.J. Park<sup>91</sup>, A. Passfeld<sup>58</sup>, B. Pastirčák<sup>51</sup>,  
D.I. Patalakha<sup>47</sup>, V. Paticchio<sup>104</sup>, B. Paul<sup>95</sup>, A. Pavlinov<sup>125</sup>, T. Pawlak<sup>124</sup>, T. Peitzmann<sup>49</sup>,  
H. Pereira Da Costa<sup>14</sup>, E. Pereira De Oliveira Filho<sup>113</sup>, D. Peresunko<sup>94</sup>, C.E. Pérez Lara<sup>77</sup>,  
D. Perini<sup>33</sup>, D. Perrino<sup>31</sup>, W. Peryt<sup>124</sup>, A. Pesci<sup>98</sup>, V. Peskov<sup>33,59</sup>, Y. Pestov<sup>5</sup>, V. Petráček<sup>37</sup>,  
595 M. Petran<sup>37</sup>, M. Petris<sup>74</sup>, P. Petrov<sup>96</sup>, M. Petrovici<sup>74</sup>, C. Petta<sup>26</sup>, S. Piano<sup>103</sup>, M. Pikna<sup>36</sup>, P. Pillot<sup>107</sup>,  
O. Pinazza<sup>33</sup>, L. Pinsky<sup>116</sup>, N. Pitz<sup>56</sup>, D.B. Piyarathna<sup>116</sup>, M. Planinic<sup>92</sup>, M. Płoskon<sup>70</sup>, J. Pluta<sup>124</sup>,  
T. Pocheptsov<sup>62</sup>, S. Pochybova<sup>126</sup>, P.L.M. Podesta-Lerma<sup>112</sup>, M.G. Poghosyan<sup>33</sup>, K. Polák<sup>53</sup>,  
B. Polichtchouk<sup>47</sup>, A. Pop<sup>74</sup>, S. Porteboeuf-Houssais<sup>66</sup>, V. Pospíšil<sup>37</sup>, B. Potukuchi<sup>85</sup>, S.K. Prasad<sup>125</sup>,  
R. Preghenella<sup>98,12</sup>, F. Prino<sup>102</sup>, C.A. Pruneau<sup>125</sup>, I. Pshenichnov<sup>48</sup>, G. Puddu<sup>23</sup>, V. Punin<sup>93</sup>,  
600 M. Putiš<sup>38</sup>, J. Putschke<sup>125</sup>, E. Quercigh<sup>33</sup>, H. Qvigstad<sup>21</sup>, A. Rachevski<sup>103</sup>, A. Rademakers<sup>33</sup>,  
T.S. Rähä<sup>42</sup>, J. Rak<sup>42</sup>, A. Rakotozafindrabe<sup>14</sup>, L. Ramello<sup>30</sup>, A. Ramírez Reyes<sup>11</sup>, R. Raniwala<sup>86</sup>,  
S. Raniwala<sup>86</sup>, S.S. Räsänen<sup>42</sup>, B.T. Rascanu<sup>56</sup>, D. Rathee<sup>82</sup>, K.F. Read<sup>118</sup>, J.S. Real<sup>67</sup>,  
K. Redlich<sup>73,iv</sup>, R.J. Reed<sup>127</sup>, A. Rehman<sup>18</sup>, P. Reichelt<sup>56</sup>, M. Reicher<sup>49</sup>, R. Renfordt<sup>56</sup>,  
A.R. Reolon<sup>68</sup>, A. Reshetin<sup>48</sup>, F. Rettig<sup>39</sup>, J.-P. Revol<sup>33</sup>, K. Reygers<sup>87</sup>, L. Riccati<sup>102</sup>, R.A. Ricci<sup>69</sup>,  
605 T. Richert<sup>32</sup>, M. Richter<sup>21</sup>, P. Riedler<sup>33</sup>, W. Riegler<sup>33</sup>, F. Riggi<sup>26,105</sup>, M. Rodríguez Cahuantzi<sup>2</sup>,  
A. Rodriguez Manso<sup>77</sup>, K. Røed<sup>18,21</sup>, D. Rohr<sup>39</sup>, D. Röhrich<sup>18</sup>, R. Romita<sup>91,106</sup>, F. Ronchetti<sup>68</sup>,  
P. Rosnet<sup>66</sup>, S. Rossegger<sup>33</sup>, A. Rossi<sup>33,28</sup>, C. Roy<sup>61</sup>, P. Roy<sup>95</sup>, A.J. Rubio Montero<sup>10</sup>, R. Rui<sup>24</sup>,  
R. Russo<sup>22</sup>, E. Ryabinkin<sup>94</sup>, A. Rybicki<sup>110</sup>, S. Sadovsky<sup>47</sup>, K. Šafařík<sup>33</sup>, R. Sahoo<sup>45</sup>, P.K. Sahu<sup>52</sup>,  
J. Saini<sup>122</sup>, H. Sakaguchi<sup>43</sup>, S. Sakai<sup>70</sup>, D. Sakata<sup>120</sup>, C.A. Salgado<sup>16</sup>, J. Salzwedel<sup>19</sup>, S. Sambyal<sup>85</sup>,  
610 V. Samsonov<sup>80</sup>, X. Sanchez Castro<sup>61</sup>, L. Šándor<sup>51</sup>, A. Sandoval<sup>60</sup>, M. Sano<sup>120</sup>, G. Santagati<sup>26</sup>,  
R. Santoro<sup>33,12</sup>, J. Sarkamo<sup>42</sup>, E. Scapparone<sup>98</sup>, F. Scarlassara<sup>28</sup>, R.P. Scharenberg<sup>89</sup>, C. Schiaua<sup>74</sup>,  
R. Schicker<sup>87</sup>, C. Schmidt<sup>91</sup>, H.R. Schmidt<sup>121</sup>, S. Schuchmann<sup>56</sup>, J. Schukraft<sup>33</sup>, T. Schuster<sup>127</sup>,  
Y. Schutz<sup>33,107</sup>, K. Schwarz<sup>91</sup>, K. Schweda<sup>91</sup>, G. Scioli<sup>27</sup>, E. Scomparin<sup>102</sup>, P.A. Scott<sup>96</sup>,  
R. Scott<sup>118</sup>, G. Segato<sup>28</sup>, I. Selyuzhenkov<sup>91</sup>, S. Senyukov<sup>61</sup>, J. Seo<sup>90</sup>, S. Serci<sup>23</sup>, E. Serradilla<sup>10,60</sup>,  
615 A. Sevcenco<sup>54</sup>, A. Shabetai<sup>107</sup>, G. Shabratova<sup>62</sup>, R. Shahoyan<sup>33</sup>, N. Sharma<sup>82,118</sup>, S. Sharma<sup>85</sup>,  
S. Rohni<sup>85</sup>, K. Shigaki<sup>43</sup>, K. Shtejer<sup>9</sup>, Y. Sibiraki<sup>94</sup>, E. Sicking<sup>58</sup>, S. Siddhanta<sup>101</sup>, T. Siemiarczuk<sup>73</sup>,  
D. Silvermyr<sup>79</sup>, C. Silvestre<sup>67</sup>, G. Simatovic<sup>59,92</sup>, G. Simonetti<sup>33</sup>, R. Singaraju<sup>122</sup>, R. Singh<sup>85</sup>,  
S. Singha<sup>122,75</sup>, V. Singhal<sup>122</sup>, B.C. Sinha<sup>122</sup>, T. Sinha<sup>95</sup>, B. Sitar<sup>36</sup>, M. Sitta<sup>30</sup>, T.B. Skaali<sup>21</sup>,  
K. Skjerdal<sup>18</sup>, R. Smakal<sup>37</sup>, N. Smirnov<sup>127</sup>, R.J.M. Snellings<sup>49</sup>, C. Søggaard<sup>76,32</sup>, R. Soltz<sup>71</sup>,  
620 H. Son<sup>20</sup>, J. Song<sup>90</sup>, M. Song<sup>129</sup>, C. Soos<sup>33</sup>, F. Soramel<sup>28</sup>, I. Sputowska<sup>110</sup>,  
M. Spyropoulou-Stassinaki<sup>83</sup>, B.K. Srivastava<sup>89</sup>, J. Stachel<sup>87</sup>, I. Stan<sup>54</sup>, I. Stan<sup>54</sup>, G. Stefanek<sup>73</sup>,  
M. Steinpreis<sup>19</sup>, E. Stenlund<sup>32</sup>, G. Steyn<sup>84</sup>, J.H. Stiller<sup>87</sup>, D. Stocco<sup>107</sup>, M. Stolpovskiy<sup>47</sup>,  
P. Strmen<sup>36</sup>, A.A.P. Suaide<sup>113</sup>, M.A. Subieta Vásquez<sup>22</sup>, T. Sugitate<sup>43</sup>, C. Suire<sup>46</sup>, R. Sultanov<sup>50</sup>,  
M. Šumbera<sup>78</sup>, T. Susa<sup>92</sup>, T.J.M. Symons<sup>70</sup>, A. Szanto de Toledo<sup>113</sup>, I. Szarka<sup>36</sup>,  
625 A. Szczepankiewicz<sup>110,33</sup>, A. Szostak<sup>18</sup>, M. Szymański<sup>124</sup>, J. Takahashi<sup>114</sup>, J.D. Tapia Takaki<sup>46</sup>,  
A. Tarantola Peloni<sup>56</sup>, A. Tarazona Martinez<sup>33</sup>, A. Tauro<sup>33</sup>, G. Tejeda Muñoz<sup>2</sup>, A. Telesca<sup>33</sup>,  
C. Terrevoli<sup>31</sup>, J. Thäder<sup>91</sup>, D. Thomas<sup>49</sup>, R. Tieulent<sup>115</sup>, A.R. Timmins<sup>116</sup>, D. Tlusty<sup>37</sup>,  
A. Toia<sup>39,28,99</sup>, H. Torii<sup>119</sup>, L. Toscano<sup>102</sup>, V. Trubnikov<sup>3</sup>, D. Truesdale<sup>19</sup>, W.H. Trzaska<sup>42</sup>,  
T. Tsuji<sup>119</sup>, A. Tumkin<sup>93</sup>, R. Turrisi<sup>99</sup>, T.S. Tveter<sup>21</sup>, J. Ulery<sup>56</sup>, K. Ullaland<sup>18</sup>, J. Ulrich<sup>63,55</sup>,  
630 A. Uras<sup>115</sup>, J. Urbán<sup>38</sup>, G.M. Urciuoli<sup>100</sup>, G.L. Usai<sup>23</sup>, M. Vajzer<sup>37,78</sup>, M. Vala<sup>62,51</sup>,  
L. Valencia Palomo<sup>46</sup>, S. Vallero<sup>87</sup>, P. Vande Vyvre<sup>33</sup>, M. van Leeuwen<sup>49</sup>, L. Vannucci<sup>69</sup>, A. Vargas<sup>2</sup>,  
R. Varma<sup>44</sup>, M. Vasileiou<sup>83</sup>, A. Vasiliev<sup>94</sup>, V. Vechernin<sup>123</sup>, M. Veldhoen<sup>49</sup>, M. Venaruzzo<sup>24</sup>,  
E. Vercellin<sup>22</sup>, S. Vergara<sup>2</sup>, R. Vernet<sup>8</sup>, M. Verweij<sup>49</sup>, L. Vickovic<sup>109</sup>, G. Viesti<sup>28</sup>, J. Viinikainen<sup>42</sup>,

Z. Vilakazi<sup>84</sup>, O. Villalobos Baillie<sup>96</sup>, Y. Vinogradov<sup>93</sup>, A. Vinogradov<sup>94</sup>, L. Vinogradov<sup>123</sup>,  
 635 T. Virgili<sup>29</sup>, Y.P. Viyogi<sup>122</sup>, A. Vodopyanov<sup>62</sup>, S. Voloshin<sup>125</sup>, K. Voloshin<sup>50</sup>, G. Volpe<sup>33</sup>,  
 B. von Haller<sup>33</sup>, I. Vorobyev<sup>123</sup>, D. Vranic<sup>91</sup>, J. Vrláková<sup>38</sup>, B. Vulpescu<sup>66</sup>, A. Vyushin<sup>93</sup>,  
 B. Wagner<sup>18</sup>, V. Wagner<sup>37</sup>, R. Wan<sup>7</sup>, Y. Wang<sup>7</sup>, Y. Wang<sup>87</sup>, M. Wang<sup>7</sup>, D. Wang<sup>7</sup>, K. Watanabe<sup>120</sup>,  
 M. Weber<sup>116</sup>, J.P. Wessels<sup>33,58</sup>, U. Westerhoff<sup>58</sup>, J. Wiechula<sup>121</sup>, J. Wikne<sup>21</sup>, M. Wilde<sup>58</sup>, G. Wilk<sup>73</sup>,  
 A. Wilk<sup>58</sup>, M.C.S. Williams<sup>98</sup>, B. Windelband<sup>87</sup>, L. Xaplanteris Karampatsos<sup>111</sup>, C.G. Yaldo<sup>125</sup>,  
 640 Y. Yamaguchi<sup>119</sup>, H. Yang<sup>14,49</sup>, S. Yang<sup>18</sup>, S. Yasnopolskiy<sup>94</sup>, J. Yi<sup>90</sup>, Z. Yin<sup>7</sup>, I.-K. Yoo<sup>90</sup>,  
 J. Yoon<sup>129</sup>, W. Yu<sup>56</sup>, X. Yuan<sup>7</sup>, I. Yushmanov<sup>94</sup>, V. Zaccolo<sup>76</sup>, C. Zach<sup>37</sup>, C. Zampolli<sup>98</sup>,  
 S. Zaporozhets<sup>62</sup>, A. Zarochentsev<sup>123</sup>, P. Závada<sup>53</sup>, N. Zaviyalov<sup>93</sup>, H. Zbroszczyk<sup>124</sup>, P. Zelniczek<sup>55</sup>,  
 I.S. Zgura<sup>54</sup>, M. Zhalov<sup>80</sup>, H. Zhang<sup>7</sup>, X. Zhang<sup>70,66,7</sup>, F. Zhou<sup>7</sup>, Y. Zhou<sup>49</sup>, D. Zhou<sup>7</sup>, H. Zhu<sup>7</sup>,  
 J. Zhu<sup>7</sup>, J. Zhu<sup>7</sup>, X. Zhu<sup>7</sup>, A. Zichichi<sup>27,12</sup>, A. Zimmermann<sup>87</sup>, G. Zinovjev<sup>3</sup>, Y. Zoccarato<sup>115</sup>,  
 645 M. Zynovyev<sup>3</sup>, M. Zyzak<sup>56</sup>

## Affiliation notes

- <sup>i</sup> Deceased
- <sup>ii</sup> Also at: M.V.Lomonosov Moscow State University, D.V.Skobeltzyn Institute of Nuclear Physics, Moscow, Russia
- 650 <sup>iii</sup> Also at: University of Belgrade, Faculty of Physics and Vinca Institute of Nuclear Sciences, Belgrade, Serbia
- <sup>iv</sup> Also at: Institute of Theoretical Physics, University of Wroclaw, Wroclaw, Poland

## Collaboration Institutes

- <sup>1</sup> A. I. Alikhanyan National Science Laboratory (Yerevan Physics Institute) Foundation, Yerevan, Armenia
- 655 <sup>2</sup> Benemérita Universidad Autónoma de Puebla, Puebla, Mexico
- <sup>3</sup> Bogolyubov Institute for Theoretical Physics, Kiev, Ukraine
- <sup>4</sup> Bose Institute, Department of Physics and Centre for Astroparticle Physics and Space Science (CAPSS), Kolkata, India
- 660 <sup>5</sup> Budker Institute for Nuclear Physics, Novosibirsk, Russia
- <sup>6</sup> California Polytechnic State University, San Luis Obispo, California, United States
- <sup>7</sup> Central China Normal University, Wuhan, China
- <sup>8</sup> Centre de Calcul de l'IN2P3, Villeurbanne, France
- <sup>9</sup> Centro de Aplicaciones Tecnológicas y Desarrollo Nuclear (CEADEN), Havana, Cuba
- 665 <sup>10</sup> Centro de Investigaciones Energéticas Medioambientales y Tecnológicas (CIEMAT), Madrid, Spain
- <sup>11</sup> Centro de Investigación y de Estudios Avanzados (CINVESTAV), Mexico City and Mérida, Mexico
- <sup>12</sup> Centro Fermi - Museo Storico della Fisica e Centro Studi e Ricerche "Enrico Fermi", Rome, Italy
- 670 <sup>13</sup> Chicago State University, Chicago, United States
- <sup>14</sup> Commissariat à l'Énergie Atomique, IRFU, Saclay, France
- <sup>15</sup> COMSATS Institute of Information Technology (CIIT), Islamabad, Pakistan
- <sup>16</sup> Departamento de Física de Partículas and IGFAE, Universidad de Santiago de Compostela, Santiago de Compostela, Spain
- 675 <sup>17</sup> Department of Physics Aligarh Muslim University, Aligarh, India
- <sup>18</sup> Department of Physics and Technology, University of Bergen, Bergen, Norway
- <sup>19</sup> Department of Physics, Ohio State University, Columbus, Ohio, United States
- <sup>20</sup> Department of Physics, Sejong University, Seoul, South Korea
- <sup>21</sup> Department of Physics, University of Oslo, Oslo, Norway

- 680 22 Dipartimento di Fisica dell'Università and Sezione INFN, Turin, Italy  
 23 Dipartimento di Fisica dell'Università and Sezione INFN, Cagliari, Italy  
 24 Dipartimento di Fisica dell'Università and Sezione INFN, Trieste, Italy  
 25 Dipartimento di Fisica dell'Università 'La Sapienza' and Sezione INFN, Rome, Italy  
 26 Dipartimento di Fisica e Astronomia dell'Università and Sezione INFN, Catania, Italy  
 685 27 Dipartimento di Fisica e Astronomia dell'Università and Sezione INFN, Bologna, Italy  
 28 Dipartimento di Fisica e Astronomia dell'Università and Sezione INFN, Padova, Italy  
 29 Dipartimento di Fisica 'E.R. Caianiello' dell'Università and Gruppo Collegato INFN, Salerno, Italy  
 30 Dipartimento di Scienze e Innovazione Tecnologica dell'Università del Piemonte Orientale and  
 690 Gruppo Collegato INFN, Alessandria, Italy  
 31 Dipartimento Interateneo di Fisica 'M. Merlin' and Sezione INFN, Bari, Italy  
 32 Division of Experimental High Energy Physics, University of Lund, Lund, Sweden  
 33 European Organization for Nuclear Research (CERN), Geneva, Switzerland  
 34 Fachhochschule Köln, Köln, Germany  
 695 35 Faculty of Engineering, Bergen University College, Bergen, Norway  
 36 Faculty of Mathematics, Physics and Informatics, Comenius University, Bratislava, Slovakia  
 37 Faculty of Nuclear Sciences and Physical Engineering, Czech Technical University in Prague, Prague, Czech Republic  
 38 Faculty of Science, P.J. Šafárik University, Košice, Slovakia  
 700 39 Frankfurt Institute for Advanced Studies, Johann Wolfgang Goethe-Universität Frankfurt, Frankfurt, Germany  
 40 Gangneung-Wonju National University, Gangneung, South Korea  
 41 Gauhati University, Department of Physics, Guwahati, India  
 42 Helsinki Institute of Physics (HIP) and University of Jyväskylä, Jyväskylä, Finland  
 705 43 Hiroshima University, Hiroshima, Japan  
 44 Indian Institute of Technology Bombay (IIT), Mumbai, India  
 45 Indian Institute of Technology Indore, Indore, India (IITI)  
 46 Institut de Physique Nucléaire d'Orsay (IPNO), Université Paris-Sud, CNRS-IN2P3, Orsay, France  
 710 47 Institute for High Energy Physics, Protvino, Russia  
 48 Institute for Nuclear Research, Academy of Sciences, Moscow, Russia  
 49 Nikhef, National Institute for Subatomic Physics and Institute for Subatomic Physics of Utrecht University, Utrecht, Netherlands  
 50 Institute for Theoretical and Experimental Physics, Moscow, Russia  
 715 51 Institute of Experimental Physics, Slovak Academy of Sciences, Košice, Slovakia  
 52 Institute of Physics, Bhubaneswar, India  
 53 Institute of Physics, Academy of Sciences of the Czech Republic, Prague, Czech Republic  
 54 Institute of Space Sciences (ISS), Bucharest, Romania  
 55 Institut für Informatik, Johann Wolfgang Goethe-Universität Frankfurt, Frankfurt, Germany  
 720 56 Institut für Kernphysik, Johann Wolfgang Goethe-Universität Frankfurt, Frankfurt, Germany  
 57 Institut für Kernphysik, Technische Universität Darmstadt, Darmstadt, Germany  
 58 Institut für Kernphysik, Westfälische Wilhelms-Universität Münster, Münster, Germany  
 59 Instituto de Ciencias Nucleares, Universidad Nacional Autónoma de México, Mexico City, Mexico  
 725 60 Instituto de Física, Universidad Nacional Autónoma de México, Mexico City, Mexico  
 61 Institut Pluridisciplinaire Hubert Curien (IPHC), Université de Strasbourg, CNRS-IN2P3, Strasbourg, France  
 62 Joint Institute for Nuclear Research (JINR), Dubna, Russia  
 63 Kirchhoff-Institut für Physik, Ruprecht-Karls-Universität Heidelberg, Heidelberg, Germany

- 730 64 Korea Institute of Science and Technology Information, Daejeon, South Korea  
65 KTO Karatay University, Konya, Turkey  
66 Laboratoire de Physique Corpusculaire (LPC), Clermont Université, Université Blaise Pascal,  
CNRS-IN2P3, Clermont-Ferrand, France  
67 Laboratoire de Physique Subatomique et de Cosmologie (LPSC), Université Joseph Fourier,  
735 CNRS-IN2P3, Institut Polytechnique de Grenoble, Grenoble, France  
68 Laboratori Nazionali di Frascati, INFN, Frascati, Italy  
69 Laboratori Nazionali di Legnaro, INFN, Legnaro, Italy  
70 Lawrence Berkeley National Laboratory, Berkeley, California, United States  
71 Lawrence Livermore National Laboratory, Livermore, California, United States  
740 72 Moscow Engineering Physics Institute, Moscow, Russia  
73 National Centre for Nuclear Studies, Warsaw, Poland  
74 National Institute for Physics and Nuclear Engineering, Bucharest, Romania  
75 National Institute of Science Education and Research, Bhubaneswar, India  
76 Niels Bohr Institute, University of Copenhagen, Copenhagen, Denmark  
745 77 Nikhef, National Institute for Subatomic Physics, Amsterdam, Netherlands  
78 Nuclear Physics Institute, Academy of Sciences of the Czech Republic, Řež u Prahy, Czech  
Republic  
79 Oak Ridge National Laboratory, Oak Ridge, Tennessee, United States  
80 Petersburg Nuclear Physics Institute, Gatchina, Russia  
750 81 Physics Department, Creighton University, Omaha, Nebraska, United States  
82 Physics Department, Panjab University, Chandigarh, India  
83 Physics Department, University of Athens, Athens, Greece  
84 Physics Department, University of Cape Town and iThemba LABS, National Research  
Foundation, Somerset West, South Africa  
755 85 Physics Department, University of Jammu, Jammu, India  
86 Physics Department, University of Rajasthan, Jaipur, India  
87 Physikalisches Institut, Ruprecht-Karls-Universität Heidelberg, Heidelberg, Germany  
88 Politecnico di Torino, Turin, Italy  
89 Purdue University, West Lafayette, Indiana, United States  
760 90 Pusan National University, Pusan, South Korea  
91 Research Division and ExtreMe Matter Institute EMMI, GSI Helmholtzzentrum für  
Schwerionenforschung, Darmstadt, Germany  
92 Rudjer Bošković Institute, Zagreb, Croatia  
93 Russian Federal Nuclear Center (VNIIEF), Sarov, Russia  
765 94 Russian Research Centre Kurchatov Institute, Moscow, Russia  
95 Saha Institute of Nuclear Physics, Kolkata, India  
96 School of Physics and Astronomy, University of Birmingham, Birmingham, United Kingdom  
97 Sección Física, Departamento de Ciencias, Pontificia Universidad Católica del Perú, Lima, Peru  
98 Sezione INFN, Bologna, Italy  
770 99 Sezione INFN, Padova, Italy  
100 Sezione INFN, Rome, Italy  
101 Sezione INFN, Cagliari, Italy  
102 Sezione INFN, Turin, Italy  
103 Sezione INFN, Trieste, Italy  
775 104 Sezione INFN, Bari, Italy  
105 Sezione INFN, Catania, Italy  
106 Nuclear Physics Group, STFC Daresbury Laboratory, Daresbury, United Kingdom  
107 SUBATECH, Ecole des Mines de Nantes, Université de Nantes, CNRS-IN2P3, Nantes, France  
108 Suranaree University of Technology, Nakhon Ratchasima, Thailand

- 780 109 Technical University of Split FESB, Split, Croatia  
110 The Henryk Niewodniczanski Institute of Nuclear Physics, Polish Academy of Sciences, Cracow,  
Poland  
111 The University of Texas at Austin, Physics Department, Austin, TX, United States  
112 Universidad Autónoma de Sinaloa, Culiacán, Mexico  
785 113 Universidade de São Paulo (USP), São Paulo, Brazil  
114 Universidade Estadual de Campinas (UNICAMP), Campinas, Brazil  
115 Université de Lyon, Université Lyon 1, CNRS/IN2P3, IPN-Lyon, Villeurbanne, France  
116 University of Houston, Houston, Texas, United States  
117 University of Technology and Austrian Academy of Sciences, Vienna, Austria  
790 118 University of Tennessee, Knoxville, Tennessee, United States  
119 University of Tokyo, Tokyo, Japan  
120 University of Tsukuba, Tsukuba, Japan  
121 Eberhard Karls Universität Tübingen, Tübingen, Germany  
122 Variable Energy Cyclotron Centre, Kolkata, India  
795 123 V. Fock Institute for Physics, St. Petersburg State University, St. Petersburg, Russia  
124 Warsaw University of Technology, Warsaw, Poland  
125 Wayne State University, Detroit, Michigan, United States  
126 Wigner Research Centre for Physics, Hungarian Academy of Sciences, Budapest, Hungary  
127 Yale University, New Haven, Connecticut, United States  
800 128 Yildiz Technical University, Istanbul, Turkey  
129 Yonsei University, Seoul, South Korea  
130 Zentrum für Technologietransfer und Telekommunikation (ZTT), Fachhochschule Worms,  
Worms, Germany